Journal of Crohn's and Colitis, 2020, 801–817
doi:10.1093/ecco-jcc/jjz188
Advance Access publication November 27, 2019
Original Article

Original Article

Prescription Opioids induce Gut Dysbiosis and Exacerbate Colitis in a Murine Model of Inflammatory Bowel Disease

Umakant Sharma,[a] Rohini Khatri Olson,[b] Federico Nicolas Erhart,[a] Li Zhang,[a] Jingjing Meng,[a] Bradley Segura,[b] Santanu Banerjee,[a,*] Madhulika Sharma,[a] Ashok Kumar Saluja,[a] Sundaram Ramakrishnan,[a] Maria T Abreu,[c] Sabita Roy[a]

[a]Department of Surgery, Miller School of Medicine, University of Miami, Miami, FL, USA [b]Department of Surgery, University of Minnesota, Minneapolis, MN, USA [c]Division of Gastroenterology, Miller School of Medicine, University of Miami, Miami, FL, USA

*Corresponding author: Sabita Roy, PhD, Department of Surgery, Miller School of Medicine, University of Miami, Miami, FL 33136, USA. Tel.: +1-305-243-8452; Email: sabita.roy@miami.edu

Abstract

Background and Aims: Opioids are the most prescribed analgesics for pain in inflammatory bowel diseases [IBD]; however, the consequences of opioid use on IBD severity are not well defined. This is the first study investigating consequences of hydromorphone in both dextran sodium sulphate [DSS]-induced colitis and spontaneous colitis (IL-10 knockout [IL-10$^{-/-}$]) mouse models of IBD.

Methods: To determine the consequences of opioids on IBD pathogenesis, wild-type [WT] mice were treated with clinically relevant doses of hydromorphone and colitis was induced via 3% DSS in drinking water for 5 days. In parallel we also determined the consequences of opioids in a spontaneous colitis model.

Results: Hydromorphone and DSS independently induced barrier dysfunction, bacterial translocation, disruption of tight junction organisation and increased intestinal and systemic inflammation, which were exacerbated in mice receiving hydromorphone in combination with DSS. Hydromorphone + DSS-treated mice exhibited significant microbial dysbiosis. Predictive metagenomic analysis of the gut microbiota revealed high abundance in the bacterial communities associated with virulence, antibiotic resistance, toxin production, and inflammatory properties. Hydromorphone modulates tight junction organisation in a myosin light chain kinase [MLCK]-dependent manner. Treatment with MLCK inhibitor ML-7 ameliorates the detrimental effects of hydromorphone on DSS-induced colitis and thus decreases severity of IBD. Similarly, we demonstrated that hydromorphone treatment in IL-10$^{-/-}$ mice resulted in accelerated clinical manifestations of colitis compared with control mice.

Conclusions: Opioids used for pain management in IBD accelerate IBD progression by dysregulation of the gut microbiota, leading to expansion of pathogenic bacteria, translocation of bacteria, immune deregulation and sustained inflammation.

Key Words: Prescription opioid, IBD, microbiome

1. Introduction

The USA is estimated to consume 80% of the global opioid supply, in spite of constituting approximately only 5% of the world's population.[1] Opioids are commonly used in the treatment of pain and associated symptoms of many diseases, including abdominal pain secondary to IBD. The uninterrupted use of opioids has been linked with adverse outcomes, including death. Attaining the required degree of analgesia often leads to tolerance due to dose escalation. A large body of studies has shown that morphine treatment induces gut barrier disruption and dysfunction of the immune system, which results in bacterial infection and ultimately sepsis.[2,3] Lately, prescription of hydromorphone for IBD pain control and associated symptoms, including diarrhoea, has increased, as it has been reported to be stronger with fewer side effects. However, the impact of hydromorphone has not been properly evaluated on alteration in gut microbiota, inflammation, and severity of disease in IBD.

IBD including ulcerative colitis [UC] and Crohn's disease [CD] affects 1.6 million people with an annual incidence of 70 000 new cases in the USA alone.[4] Although the pathogenesis of IBD remains complex, immune dysfunction, host genotype, environmental exposure, lifestyle factors and, more recently, compositional changes in enteric microbiome are increasingly implicated in disease pathophysiology.[5,6] The interactions between intestinal epithelial damage and microbial dysbiosis are proving to be the most potent host factors in the pathogenesis of the disease.[7,8] IBD is associated with severe morbidity and impaired quality of life owing to its chronic nature and high recurrence, and represents a substantial socioeconomic burden in the USA costing approximately over two billion dollars annually.[4,9,10]

IBD pathogenesis involves damage to the gut epithelial layer and dysregulation of immune response to intestinal microbes.[5] Among various animal models, dextran sulphate sodium [DSS]-induced colitis and spontaneous colitis [IL-10$^{-/-}$] are the most extensively used and best described murine models of IBD.[11–13] In the DSS model, mice are treated with 3–5% DSS in their drinking water for 5–9 days to induce acute colitis,[14–16] which provides a model of acute intestinal injuries which permits clinical monitoring of colitis.[17] The macroscopic signs, as well as microscopic observations, in a murine model recapitulate many aspects of IBD in humans.[11]

The intestinal microbiota is associated with fundamental physiological processes.[18] The gut microbiota mostly consists of Gram-positive Firmicutes and Gram-negative Bacteroidetes, which are conserved in humans and mice.[19] Gut microbial dysbiosis is commonly associated with IBD. There is growing evidence that dysregulated immune response against commensal bacteria leads to IBD, and the enormous variety of gut flora contributes to the heterogeneity of the disease. IBD patients show higher numbers of Proteobacteria and lower numbers of Firmicutes with reduced functional diversity compared with healthy individuals.[20]

IBD is an independent risk factor in heavy opioid users. Patients with IBD have abdominal pain that is not infrequently medicated with opioids, especially in the hospital setting. Approximately 15% of IBD patients are on chronic opioids and an estimated 5% of individuals become dependent, which is associated with a significant risk of mortality.[21] Previous studies in our laboratory show that morphine causes disruption of intestinal tight junction proteins organisation and gut barrier dysfunction, induces bacterial translocation, and modulates immune responses.[3] Opioid use has been linked with increased complications, hospitalisations, decreased quality of life, and mortality in IBD patients[22,23] but in clinical care it is difficult to assess whether opioid use is associated with the more inflamed patients or whether opioids worsen intestinal inflammation.

Based on our previous studies, we hypothesised that prescription opioids will worsen intestinal inflammation and thus severity of IBD. We investigated the integrity of intestinal tight junction proteins organisation, gut barrier dysfunction, and microbial dysbiosis as potential underlying mechanisms. To test our hypothesis and to determine if opioids can independently impact on the severity of the disease, we investigated the consequence of the prescription opioid, hydromorphone, on: gut barrier dysfunction; disruption of tight junction proteins organisation affecting intestinal epithelial cells; microbial dysbiosis; and intestinal as well as systemic inflammation in both DSS colitis and IL-10$^{-/-}$ mouse model of IBD. Tight junction proteins maintain intestinal barrier integrity. The tight junction includes paracellular proteins such as Zona occludens-1 [ZO-1] and transmembrane protein such as claudin-1, which assist to seal the paracellular pathway between adjacent intestinal epithelial cells. Previous studies have shown that tight junction disruption is initiated by the phosphorylation of the myosin light chain [MLC], which mainly depends on activation of MLCK. It has been shown that there is strong association between gut barrier dysfunction and toll-like receptor [TLR] activation.[3] However, the mechanisms underlying disruption of tight junction integrity after hydromorphone treatment are not well defined. Disruption of intestinal tight junction barrier function has severe consequences, including bacterial translocation from the gut leading to immune activation and inflammation. Therefore, for the first time we elucidated the mechanism by which hydromorphone alters intestinal tight junctions organisation in a murine model of IBD. Our results indicate that hydromorphone-induced MLCK-dependent disruption of intestinal tight junction proteins mediates epithelial barrier dysfunction, which in turn increases the severity of IBD. Selective inhibition of MLCK activation attenuates opioid-induced exacerbation of IBD. The results of this study provide a new perspective on the effects of opioid on IBD pathogenesis.

2. Methods

2.1. Experimental animals

We used pathogen-free wild-type [WT] *C57BL/6* [stock no: 000664] and interkeukin-10 knockout [IL-10$^{-/-}$] *C57BL/6* [stock no: 002251] male mice 10–16 weeks old [Jackson Laboratory, CA, USA]. Mice were kept under standardised conditions at 22 ± 2℃ and 50% humidity, under a 12-h light/dark cycle, and were maintained with *ad lib* access to standard chow and tapwater. Acclimation to the laboratory conditions occurred for at least 7 days before experimental inclusion.[19,24]

2.2. Animal treatment

The animals were treated with a clinically relevant dose range of hydromorphone 0.53 mg–1.2 mg/kg/day, which was calculated to be equivalent to 1.25–7.5 mg/kg twice daily [bid] in mice[25–27] by intraperitoneal injection [IP]. The conversion of human to mouse dose was done based on the surface area of the mouse.[28,29] After 48 h of treatment, the mice were euthanised and evaluated for the consequences of hydromorphone. In this approach, the most effective dose of hydromorphone [7.5 mg/kg bid] was selected on the basis of dose-response experiments for evaluating the consequences of hydromorphone on the severity of DSS-induced colitis in a murine model of IBD. Further mice were treated with saline [Control], hydromorphone [H], DSS [DSS], and hydromorphone

plus DSS [H+DSS]. While hydromorphone was continued, at Day 3 acute colitis was induced by oral administration of 3% DSS [molecular weight: MW 40 kDa; MP Biomedicals, Soho, OH, USA] dissolved in drinking water for 5 days. The milder DSS for short duration treatment model is a powerful means of evaluating the effect of hydromorphone on the severity of colitis in a murine model of IBD. To evaluate the effect of MLCK inhibitor ML-7 on intestinal tight junction proteins organisation and severity of colitis in hydromorphone- and DSS-treated mice, the most widely used dose of ML-7 [2 mg/kg] was used. Animals were injected with ML-7 intraperitoneally twice a day for 8 days.[3,30] The untreated mice served as control and received normal drinking water.[19,31]

2.3. Measurement of body weight and colon length

The mice body weight was measured on Day 0 [initial weight] and Day 7 [final weight] and the weight loss was determined. After 7 days, mice were euthanised and the entire colon was removed and measured in centimetres to determine the colon length of control and of treated mice.[11,31]

2.4. Endoscopic examination of colon

On Day 7, the endoscopy was performed to evaluate DSS-induced colonic destruction using the Coloview system [Karl Storz Veterinary Endoscopy, Tuttlingen, Germany]. The endoscopic procedure was viewed and digitally recorded. Colonoscopic score was given by assessing different colonic features including translucency, presence of fibrin, granularity, mucosal vascular pattern [MVP] loss, stool characteristics, and presence of blood. For each category, a score of 0 indicated normal, 1 indicated mild change, 2 indicated moderate change, and 3 indicated severe change. The combined colonoscopic score ranged from 0 [normal appearance] to 18 [severe damage and inflammation] and was determined in similar fashion, as mentioned.[11]

2.5. Gut permeability assay

To evaluate the gut leakiness, mice were gavaged with rhodamine B isothiocyanate-dextran [MW 70kDa, Sigma-Aldrich] at the dose of 600 mg/kg body weight of mouse. After 3–4 h, fluorescence intensity in plasma of the mice was measured using a Fluorometer [Thermo Scientific™] with an excitation/emission wavelength of 570/590 nm.

2.6. Histological analysis

To examine the impact of hydromorphone on severity of colitis, mouse colon tissue was harvested from the distal colon [-cm from the rectum] and was cut into segments. The tissue was fixed with 10% formaldehyde overnight, embedded in paraffin, sectioned at 5 µm, mounted on clean glass slides, and stained with haematoxylin and eosin [H&E] for histological evaluation. The H&E-stained samples were randomised and coded, to perform unbiased histological evaluation. The slides were analysed in a blinded fashion by a pathologist using light microscopy. Each sample was given a histological score based on cumulative scores specified to different histological features, including degree of epithelial damage or tissue destruction, loss of crypt and villus architecture, inflammatory cell infiltration, and ulceration or oedema. For each category, a score of 0 indicated normal appearance, a score of 1 indicated mild change, and a score of 2 indicated severe change, encompassing greater than 50% of the high-power field. The combined histological score ranged from 0 [normal appearance] to 8 [extensive tissue damage and inflammatory cell infiltration] and was determined in similar fashion, as mentioned in previous studies.[19,31]

2.7. Bacterial translocation

After necropsy, liver tissue was harvested and homogenised in sterile phosphate-buffered saline [PBS] using 100-µm cell strainers [BD Biosciences], following aseptic techniques. Homogenised tissue was then plated on blood agar plates and incubated at 37°C overnight in aerobic conditions. Bacterial colonies were counted as colony-forming units [CFU] and normalised for varying protein concentrations in the tissue homogenate.

2.8. Cytokine level measurement

Liver tissue was homogenised and suspended in PBS containing protease inhibitors [Sigma]. Supernatants were collected after centrifugation [10 000 rpm for 5 min] and the levels of cytokines such as IL-6 and IL-17A were determined using enzyme-linked immunosorbent assay [ELISA, eBiosciences].[19]

2.9. Immunofluorescence staining and image analysis

The fixed colon sections were deparaffinised with xylene and rehydrated through a series of graded alcohols, and then processed for antigen retrieval. These processed sections of colonic tissue were used for macrophage and tight junction staining. For macrophage staining, tissues were incubated with fluorescein isothiocyanate isomer 1 [FITC]-conjugated anti-mouse F4/80 antibody [BD Biosciences, USA] at a 1:100 dilution in PBS overnight at 4℃, followed by counterstaining with DAPI. ImageJ [National Institute of Health] software was used to quantify the number of macrophages.

The colon sections were also stained for ZO-1 and claudin-1, two proteins integral to the formation of epithelial tight junction. For tight junction staining, tissue sections were incubated with polyclonal rabbit antibody against ZO-1 or claudin-1 [Invitrogen] in PBS with 1% bovine serum albumin [BSA] overnight at 4℃. After washing, sections were incubated with rhodamine phalloidin [Invitrogen] and secondary Alexa Fluor 488-conjugated goat anti-rabbit IgG antibody [Invitrogen] for 1 h at room temperature. After washing thrice in PBS, sections were mounted under coverslips using ProLong Gold antifade reagent with DAPI [Invitrogen]. Sections were imaged and photographed using a laser confocal microscope [Leica Microsystems, Germany]. ImageJ [National Institute of Health] software was used to image processing and quantify the green fluorescence intensity, which was normalised to area.[32]

2.10. Microbiota analysis using bacterial 16s rDNA amplification and miseq250 sequencing

Enteric content [faecal material] was collected from the distal colon region and frozen on dry ice. The DNA was isolated using Powersoil/faecal DNA isolation kit [Mo Bio Laboratories, Inc.] as per manufacturer's specifications. All DNA samples were quantified using Qubit® Quant-iT dsDNA Broad- Range Kit [Invitrogen, Life Technologies, Grand Island, NY] and submitted to the University of Minnesota Genomic Center for sequencing of the bacterial 16S V5-V6 rDNA region.[33] Resulting sequences were then searched against the Greengenes reference database of 16S sequences, clustered at 97% by UCLUST [closed-reference OTU picking]. The microbiome data were analysed using QIIME at the phyla and lower taxonomic levels.[34]

2.11. Microbiome phenotype analysis

Predicted metagenomic functional analysis based on microbial communities using 16s rDNA marker gene sequences was performed[35] by using a BugBase software package, which is based on the softwares

like PICRUSt, QIIME,[36] and KEGG metabolic operational taxonomic units [OTUs] from the GreenGenes reference database.[37]

2.12. Quantitative real-time polymerase chain reaction

Total RNA from colon tissue was isolated using TRIzol [Invitrogen] method. The cDNA was synthesizsd using High-Capacity cDNA Reverse Transcription Kit [Applied Biosystems]. The changes in host gene expression were measured using gene-specific primers for mu opioid receptor [MOR], TLR2, TLR4, and glyceraldehyde-3-phosphate dehydrogenase [GAPDH] from Invitrogen. Quantitative real-time polymerase chain reaction [qPCR] was performed using LightCycler® 96 Real-Time PCR System [Roche], and mRNAs were quantified using SYBR green Master Mix as directed by the manufacturer's protocol. All samples were run in triplicate, and relative mRNA expression levels were determined after normalising all values to the unaffected housekeeping gene GAPDH as the reference.

2.13. Statistics

All results are presented as mean ± standard error of the mean [SEM]. Data were analysed using GraphPad Prism 8 statistical software, and p <0.05 was considered as statistically significant. Statistical comparison among more than two groups was analysed using one-way analysis of variance [ANOVA] followed by Tukey's multiple comparisons test.

2.14. Study approval

All animal experiments were approved by the Institutional Animal Care and Use Committee [IACUC], University of Minnesota and University of Miami. The experiments were performed in compliance with the institutional laws and guidelines.

3. Results

Hydromorphone induces weight loss, intestinal permeability, and bacterial translocation in a dose-dependent manner

We investigated whether hydromorphone treatment perturbs fundamental aspects of IBD pathogenesis in mice. The animals were treated with clinically relevant doses of hydromorphone [1.25–7.5 mg/kg twice daily] to determine the most effective treatment dose of hydromorphone for subsequent experiments in the DSS-induced colitis mouse model.

To determine the effect of hydromorphone on change in body weight, the initial and final body weight was measured for all mice in five experimental groups. No mortality was observed in any of the groups for the duration of the study. Hydromorphone treatment resulted in significant loss in body weight in a dose-dependent manner. All mice in the treatment groups showed significant body weight loss, and the highest weight loss score of 16.18 ± 0.74 was recorded with the highest dose of hydromorphone [7.5 mg/kg twice daily] compared with the control group (95% confidence interval [CI] 13.84–18.52, p <0.0001] [Figure 1A].

To investigate the consequence of hydromorphone on intestinal permeability, we assessed gut leakiness by measuring the leakage of orally administered rhodamine B fluorescence level in blood plasma using a fluorometer. The lower dose of hydromorphone [2.5 mg/kg twice daily] showed significant fluorescence level of 4.03 ± 0.41 [95% CI 2.71–5.34, p = 0.0014] compared with control, and the highest fluorescence 5.44 ± 0.65 [95% CI 3.38–7.49, p <0.0001] was recorded at highest dose of hydromorphone [7.5 mg/kg twice daily] compared with control groups. The fluorescence levels in blood plasma samples are shown in Figure 1B. The results show dose-dependent significant increase in gut permeability following hydromorphone treatment. Highest permeability was seen at the highest dose of hydromorphone, compared with control mice.

To determine the consequence of gut permeability as bacterial translocation from gut to systemic compartments of the body, liver was isolated, homogenised, and cultured on blood agar plates overnight in aerobic conditions. The bacterial colonies were counted as colony-forming units [CFU] and normalised per milligram of total protein of liver tissue homogenate. The hydromorphone-treated mice showed significant bacterial translocation compared with control mice [Figure 1C]. The highest number of colonies at 77 ± 7.18 [95% CI 54.16–99.84, p <0.0001] was observed in mice treated with the highest dose of hydromorphone compared with the control group.

3.1. Hydromorphone worsens clinical symptoms of colitis

We next asked whether hydromorphone worsens clinical symptoms of colitis and increases severity of the disease in a mouse model of IBD. To evaluate the effect of hydromorphone on severity of colitis, the most effective dose of hydromorphone [7.5 mg/kg twice daily] was used for further study in a DSS mouse model. All groups with DSS treatment

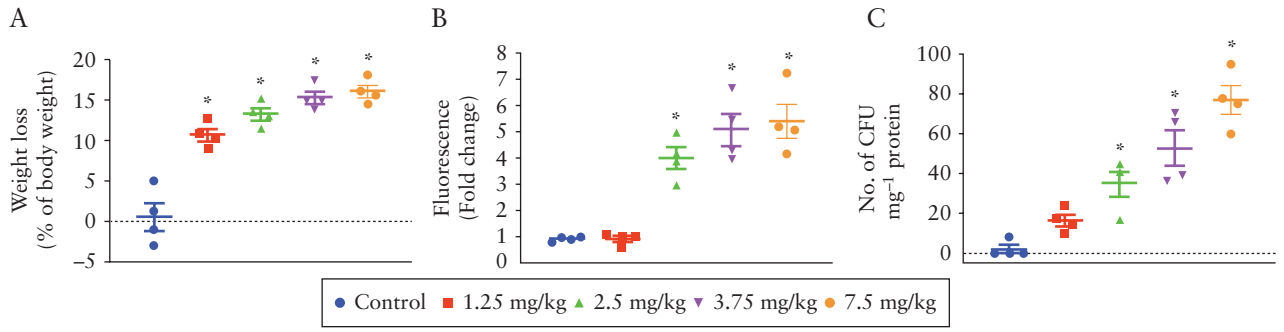

Figure 1. Hydromorphone treatment perturb fundamental aspects of inflammatory bowel disease [IBD pathogenesis in mice in a dose-dependent manner. Hydromorphone treatment induces body weight loss, gut permeability, and bacterial translocation. [A] Changes in body weight [n = 4 per group]. [B] Measurement of rhodamine B fluorescence level in plasma of hydromorphone-treated and control mice show degree of intestinal permeability [n = 4 per group]. [C] Bacterial translocation. Liver was isolated, homogenised, and cultured on blood agar plate overnight and colony-forming units [CFU] were counted [n = 4 per group]. Mean ± standard error of the mean [SEM], 95% confidence interval [CI]. Asterisk [*] indicates statistical significance [p <0.05] vs control group. and hash sign [#] indicates statistical significance [p <0.05] between treatment groups by analysis of variance [ANOVA] followed by Tukey's multiple comparisons test.

exhibited an increase in diarrhoea and rectal bleeding from Day 3 post-DSS until completion of the experiment. No mortality was observed in any of the groups for the duration of the study. All animals in the treatment groups showed significant loss in body weight compared with control, and the weight loss was significantly higher at 14.16 ± 1.16 [95% CI 11.32–16.99, p <0.0001] in the hydromorphone plus DSS-treated group compared with DSS treatment alone [Figure 2A]. No significant difference in DSS consumption was found between the groups.

On Day 7, colonoscopy was performed to evaluate colon characteristics. The representative images of colonoscopy examination from each group are shown in Figure 2B. The colonoscopy examination showed that hydromorphone plus DSS-treated mice displayed greater loss in translucency, fibrin, granularity, and mucosal vascular pattern [MVP] with increased bleeding and diarrhoea, compared with hydromorphone or DSS alone. Colonoscopy score was evaluated based on different colon characteristics, and hydromorphone plus DSS-treated mice showed significantly higher score at 14.93 ± 0.46 [95% CI 13.81–16.04, p <0.0001] compared with the DSS treatment group [Figure 2B]. Colon length measurement is a useful assessment of colitis and it is considered as a marker of inflammation. The representative images of colon length shortening, an indicator of the severity of colitis, following 5 days after DSS administration, are shown in Figure 2C. The colon length of all mice in each group was measured in centimetres [cm] and is shown in Figure 2C. A significant decrease in colon length 5.71 ± 0.20 [95% CI 5.23–6.20, p = 0.0304] was observed in hydromorphone plus DSS treated animals compared with DSS alone [Figure 2C].

3.2. Hydromorphone enhances gut permeability and bacterial translocation in DSS-treated mice

To determine the effect of hydromorphone and DSS on intestinal barrier function, we assessed gut permeability by oral administration of 70-kDa rhodamine B and measuring the leakage of rhodamine B fluorescence level in blood plasma after 4 h, using a fluorometer. The quantitative measurement of rhodamine B fluorescence levels showed that gut permeability was increased in treated mice compared with control. Significantly higher levels of rhodamine B fluorescence were observed in all treated groups and it was highest at 10.23 ± 0.76 [95% CI 8.37–12.08, p <0.0001] in hydromorphone plus DSS-treated mice [Figure 3A].

We hypothesised that compromised gut permeability in treated mice may play a role in intestinal bacterial translocation systemically. Increase in the translocation of bacteria was observed in the liver of animals that were treated with either hydromorphone or DSS alone, but significantly high levels of CFU at 1039 ± 274.5 [95% CI 366.8–1710, p = 0.0051] were observed in animals that were treated with both hydromorphone and DSS, when compared with individually treated groups [Figure 3B].

3.3. Hydromorphone exacerbates DSS-induced intestinal inflammation and immune cell infiltration

We next evaluated histologically the haematoxylin and eosin [H&E]-stained sections of the distal colon in untreated and treated animals. No histopathological changes were found in the control group, whereas hydromorphone- and DSS-treated animals showed irregularity, crypt distortion, extensive mucosal damage with large numbers of inflammatory cell infiltrates, mucus discharge, and architectural abnormalities in crypts. In the hydromorphone plus DSS-treated animals, inflammatory immune cell infiltration was widespread and severe epithelial damage was evident with complete crypt disappearance, shortening of glands, granular hyperplasia, oedema, and mucosal erosion in some areas [Figure 3C], resulting in the highest histological score by microscopic analysis. The occurrence of IBD was corroborated based on histological damage and inflammatory infiltrate into the colon. In the hydromorphone and DSS groups, preparations showed grade 0, 1, and 2 lesions, which were graded based on colon characteristics and presented as histological scores. The histological score in hydromorphone plus DSS-treated animals was

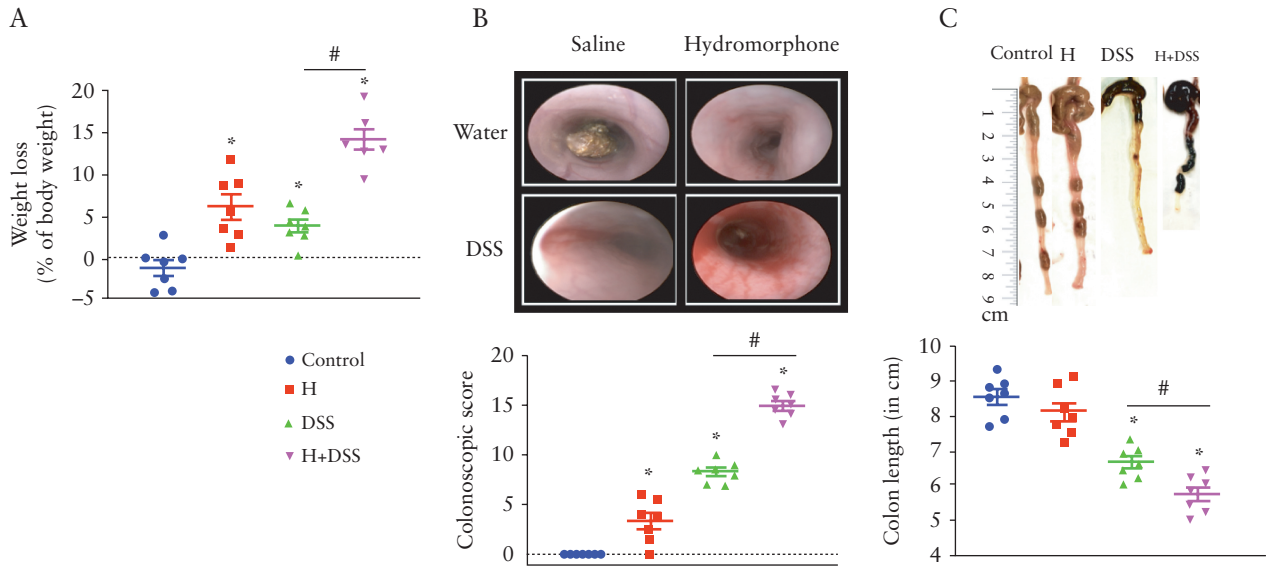

Figure 2. Hydromorphone worsens clinical symptoms of colitis and increase severity of the disease. [A] Body weight loss after DSS challenge in hydromorphone-treated and non-treated mice. Control mice received water alone [n = 7 per group]. [B] Representative images of colonoscopic examination. Colonoscopy score was calculated by assessing various characteristic with maximum score of 18 in control and treated mice [n = 7 per group]. [C] Colon length shortening. Representative images of the colon from each group and colon length was measured [n = 7 per group]. Mean ± SEM, 95% CI. Asterisk [*] indicates statistical significance [p <0.05] vs control group and hash sign [#] indicates statistical significance [p <0.05] between treatment groups by ANOVA followed by Tukey's multiple comparisons test. DSS, dextran sulphate sodium; SEM, standard error of the mean; CI, confidence interval; ANOVA, analysis of variance.

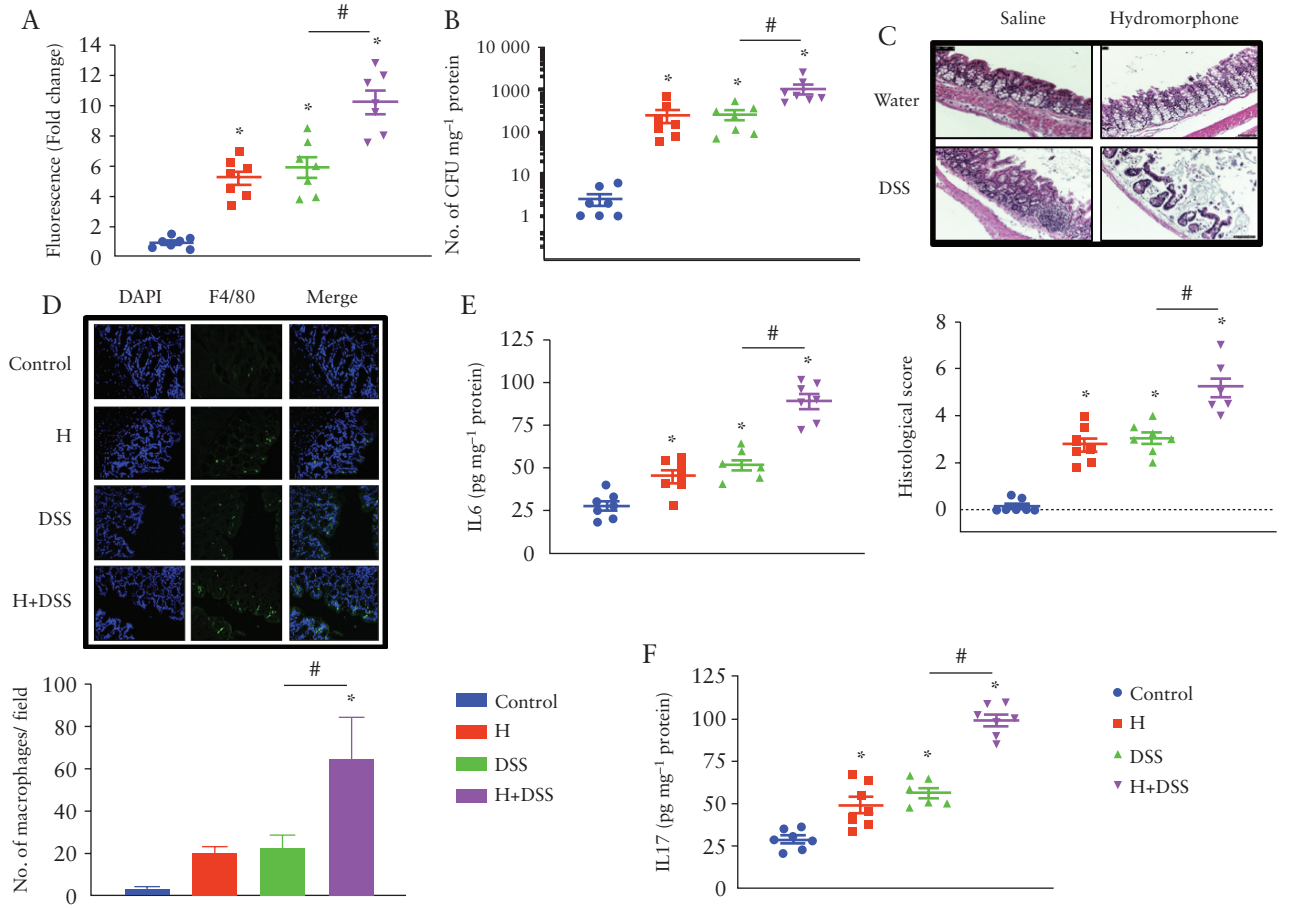

Figure 3. Hydromorphone induces gut permeability and enhances intestinal and systemic inflammation in DSS-treated mice. [A] Measurement of rhodamine B fluorescence level in plasma of treated and control mice shows degree of intestinal permeability [$n = 7$ per group] [B] Bacterial translocation [$n = 7$ per group]. [C] Representative images of H&E-stained sections of the colon from control and treated mice. Scale bar: 50 μm [original magnification: x 20] [$n = 7$ per group]. Histological scoring was done based on different histopathological features and histopathological changes were scored in a blinded fashion by a pathologist. [D] Representative images of immunohistochemical staining for macrophages in the colon using F4/80 antibody and quantitative measurement of macrophages. The number of F4/80-positive macrophages in the colon of hydromorphone + DSS treated mice is more than that of control, of hydromorphone alone- and of DSS alone-treated mice Scale bar: 50 μm [original magnification: x 20] [$n = 7$ per group]. [E] The concentrations of IL-6 [$n = 7$ per group] and [F] IL-17 in the liver homogenate were measured using ELISA [$n = 7$ per group]. Mean ± SEM, 95% CI. Asterisk [*] indicates statistical significance [$p < 0.05$] vs control group and hash sign [#] indicates statistical significance [$p < 0.05$] between treatment groups by ANOVA followed by Tukey's multiple comparisons test. DSS, dextran sulphate sodium; H&E, haematoxylin and eosin; ELISA, enzyme-linked immunosorbent assay; SEM, standard error of the mean; CI, confidence interval; ANOVA, analysis of variance.

significantly higher at 5.21 ± 0.39 [95% CI 4.26–6.17, $p < 0.0001$] compared with control and individually treated groups [Figure 3C]. We next determined the cell type of inflammatory infiltrate into the colon by immunofluorescence staining of colon sections. The representative images of our immunofluorescence staining analysis showed intestinal inflammation and infiltration of immune cells into the colon. We also quantified the number of migrated macrophages into the colon. Notably, 5 days after the DSS challenge, the numbers of macrophage mobilisation and accumulation in the colon were significantly higher in hydromorphone plus DSS-treated mice at 65 ± 19.33 [95% CI 17.69–112.3] compared with control [$p = 0.0013$] and individually treated animals [$p = 0.0341$] [Figure 3D].

3.4. Hydromorphone increases systemic pro-inflammatory cytokine levels and worsens inflammation in DSS-induced colitis

We next asked whether hydromorphone induces cytokines production systemically and further increases levels of cytokines in DSS-treated mice. The levels of cytokines were measured in the supernatant of liver homogenate using ELISA. Hydromorphone- and DSS-treated mice displayed significantly elevated levels of IL-6 [Figure 3E] and IL-17A [Figure 3F] compared with control. The levels of IL-6 at 89.58 ± 4.32 [95% CI 79.01–100.1, $p < 0.0001$] and IL-17A at 99.22 ± 3.46 [95% CI 90.76–107.7, $p < 0.0001$] were highest in hydromorphone plus DSS-treated animals compared with DSS alone.

3.5. Hydromorphone treatment accelerates development of colitis in IL-10$^{-/-}$ mice

After determining that hydromorphone worsens clinical symptoms of colitis and increases severity of the disease in the DSS-induced colitis model of IBD, we further validated the consequences of hydromorphone in a spontaneous colitis mouse model [IL-10$^{-/-}$ mouse]. The consequences of hydromorphone treatment on clinical symptoms of colitis were evaluated in an independent experiment in which the effect of hydromorphone on WT mice was reproduced with similar results as described previously [Figures 1, 2, and 3]. Treatment of IL-10$^{-/-}$ mice with hydromorphone [7.5 mg/kg twice daily] for 7

days resulted in accelerated clinical manifestations of colitis compared with control IL-10$^{-/-}$ mice receiving normal saline. Hydromorphone-treated IL-10$^{-/-}$ mice showed significant loss in average body weight of 3.2 ± 1.40 [95% CI 0.09–6.38, p = 0.0002] compared with control IL-10$^{-/-}$ mice. Reduced weight gain was also observed in hydromorphone-treated WT mice compared with WT control mice who received normal saline [p <0.0001] [Figure 4A]. The representative images of colon length shortening are shown in Figure 4B. A significant decrease in colon length was observed in hydromorphone-treated IL-10$^{-/-}$ mice at 6.23 ± 0.12 [95% CI 5.96–6.50] compared with IL-10$^{-/-}$ [p = 0.0038] and WT [p <0.0001] controls [Figure 4B]. In the DSS colitis model, we demonstrated that compromised gut permeability plays a role in intestinal bacterial translocation systemically. Significant increase in the translocation of bacteria was also observed in the liver of IL-10$^{-/-}$ mice that were treated with hydromorphone compared with IL-10$^{-/-}$ control group at 384 ± 36.67 [95% CI 301–467, p = 0.0003] [Figure 4C]. No histopathological changes were found in the WT control group, whereas hydromorphone-treated animals showed extensive mucosal damage with large numbers of inflammatory cell infiltrates, mucus discharge, and architectural abnormalities in crypts. In the hydromorphone-treated IL-10$^{-/-}$ mice, inflammatory immune cells infiltration was widespread, and epithelial damage was evident with complete crypt disappearance and mucosal erosion in some areas [Figure 4D]. The histology score of hydromorphone-treated WT at 2.56 ± 0.28 [95% CI 1.91–3.20] and IL-10$^{-/-}$ at 5.17 ± 0.26 [95% CI 4.56–5.77] mice was significantly higher compared with WT [p <0.0001] and IL-10$^{-/-}$ controls [p <0.0001] [Figure 4D]. Hydromorphone-treated WT and IL-10$^{-/-}$ mice also displayed significantly elevated levels of IL-6 compared with WT at 59.68 ± 5.84 [95% CI 46.47–72.89, p = 0.0012] and IL-10$^{-/-}$ at 124.8 ± 7.70 [95% CI 107.4–142.2, p <0.0001] controls [Figure 4E], respectively. Similarly, hydromorphone-treated WT and IL-10$^{-/-}$ mice showed significantly elevated levels of IL-17A compared with WT at 132 ± 9.99 [95% CI 109.4–154.6, p = 0.0007] and IL-10$^{-/-}$ 173.5 ± 13.27 [95% CI 143.5–203.5, p = 0.0106] controls [Figure 4F].

3.6. Hydromorphone induces microbial dysbiosis and decreases bacterial diversity in DSS-treated mice

The results of our initial study support the hypothesis that hydromorphone perturbs gut homeostasis. Therefore, further we

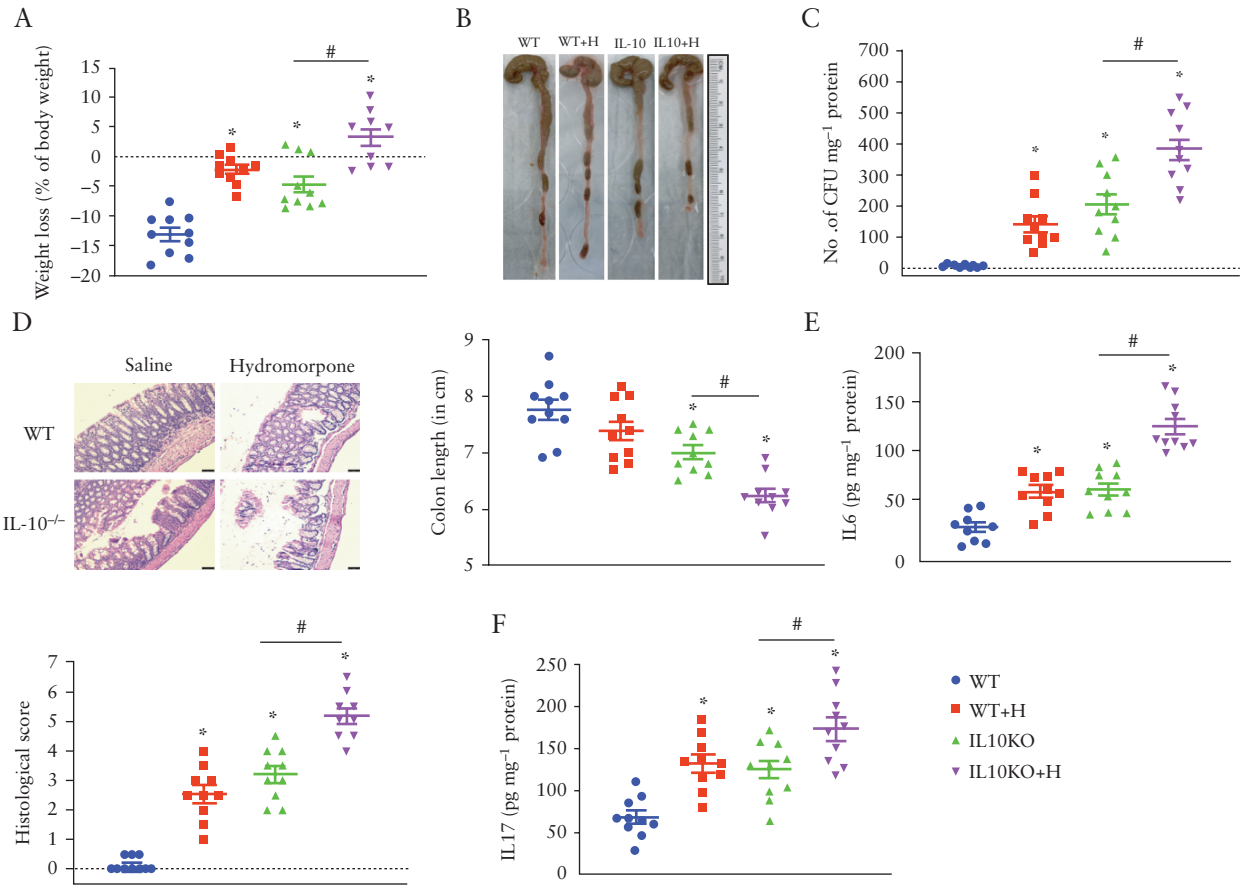

Figure 4. Hydromorphone induces inflammation and accelerates clinical manifestations of colitis in IL-10 KO mice. [A] Body weight loss in hydromorphone-treated and non-treated IL-10 KO mice. Control mice received saline [n = 10 per group]. [B] Colon length shortening. Representative images of the colon from each group and colon length was measured [n = 10 per group]. [C] Bacterial translocation [n = 10 per group]. [D] Representative images of H&E-stained sections of the colon from control and treated mice. Scale bar: 50 μm [original magnification: x 20] [n = 10 per group]. Histological scoring was done based on different histopathological features and histopathological changes were scored in a blinded fashion by a pathologist. [E] The concentration of IL-6 [n = 10 per group] and [F] IL-17 in the liver homogenate were measured using ELISA [n = 10 per group]. Mean ± SEM, 95% CI. Asterisk [*] indicates statistical significance [p <0.05] vs control group and hash sign [#] indicates statistical significance [p <0.05] between treatment groups by ANOVA followed by Tukey's multiple comparisons test. H&E, haematoxylin and eosin; ELISA, enzyme-linked immunosorbent assay; SEM, standard error of the mean; CI, confidence interval; ANOVA, analysis of variance.

investigated whether these perturbations increase the severity of DSS-induced colitis. The intestinal contents were collected for 16S rDNA sequencing to study gut microbiota. We determined gut microbial changes in each group of mice to establish a link between microbial dysbiosis, hydromorphone, and DSS-induced colitis in mice. Principal component analysis was used to evaluate composition of the intestinal microbiota. Correlations between the resulting changes in microbial composition and susceptibility to DSS-induced colitis identified signature bacterial families regulating the severity of colitis. Alpha-diversity analysis, which describes observed numbers of bacterial species richness within a community, was done by Chao 1 using QIIME workflow. The result showed significant reduction in alpha diversity and species richness in the gut bacterial community in the hydromorphone plus DSS-treated group compared with control and individually treated mice [Figure 5A]. Beta diversity analysis, which describes observed numbers of species richness between communities, was done by principal component analysis [PCoA] of resulting distance matrices to generate three-dimensional plots using QIIME. The result showed distinct clustering of the microbial community based on the treatment groups, suggesting that all four treatment group contained distinct microbial communities [Figure 5B]. The unweighted UniFrac distance was calculated using standardised galaxy and QIIME[34] at the Minnesota Supercomputing Institute [University of Minnesota, Minneapolis, MN, USA]. The result showed significant unifrac distance between the DSS alone and hydromorphone plus DSS-treated groups [Figure 5C], suggesting treatment with hydromorphone mediating the reduction in bacterial species richness and contributing to distinct bacterial communities.

3.7. Hydromorphone alters microbial composition at the phyla and lower taxonomic levels

Microbial composition analysis was performed on phylum to genus levels to identify the bacterial taxa, which are altered and may enhance severity of colitis in hydromorphone-treated DSS mice. Global analysis of the microbiota at phylum level demonstrated a total of 9 bacterial phyla, of which four were more abundant, including Firmicutes, Bacteroidetes, Proteobacteria, and Verrucomicrobia, and five were less abundant, including Actinobacteria, Deferribacteres, Tenericutes, cyanobacteria and TM7. Hydromorphone treatment significantly altered the composition of gut microflora in DSS-treated mice. The bacterial phylum Firmicutes was under-represented and Proteobacteria and Verrucomicrobia were over-represented in hydromorphone plus DSS-treated animals compared with controls [Figure 5D]. On the other hand, the OTU abundance analysis shows significant decrease in Firmicutes and significant increase in Proteobacteria and Verrucomicrobia phyla in hydromorphone plus DSS-treated mice compared with control and individually treated mice [Figure 5D]. The progression of colitis did not affect Bacteroidetes significantly.

Classification of the OTUs at the lower taxonomical levels resulted in identification of many taxa. At the family level, taxonomic analyses show increased abundance of Bacteroidaceae, Porphyromonadaceae, Enterococcaceae, Enterobacteriaceae, Verrucomicrobiaceae, and Peptostreptococcaceae, whereas reduced abundance was observed of Odoribacteraceae, Rikenellaceae, S24-7, Lactobacillaceae, Lachnospiraceae, and Ruminococcaceae in hydromorphone treated DSS-mice compared with control mice [Figure 5E]. Bacteroidaceae expanded to represent the major bacterial family. The abundance of Enterobacteriaceae correlated with the magnitude of colitis. Taxonomic analysis at the genus level showed expansion of Bacteroides, Parabacteroides, Enterococcus, Turicibacter, Ruminococcus, Sutterella, Bilophila, and Akkermansia, but depletion of Adlercreutzia, Odoribacter, AF12, Lactobacillus, and Anaerostipes in hydromorphone plus DSS-treated mice compared with control mice [Figure 5F]. The analysis indicated that Shutterella accounted for the observed increase of Enterobacteriaceae, Bacteroides for Bacteroidaceae, and Akkermansia for Verrucomicrobiaceae. The species level analyses show elevation of *Bacteroides acidifaciens*, *Ruminococcus gnavus*, and *Akkermansia muciniphila*, but contraction of *Mucispirillum schaedleri* and *Lactobacillus reuteri* in hydromorphone-treated DSS mice compared with control mice.

3.8. Hydromorphone induces functional pathogenicity and anti-microbial resistance

Phylogenetic marker [16S rRNA] gene profiling is a crucial technique to study microbial communities, but does not provide indications about functional consequences of intervention in the community. To further measure the functional composition or phenotypes following intestinal microbial dysbiosis, predicted metagenomic functional analysis was performed using a BugBase software package. BugBase analysis is a computational approach that relies on 16S rRNA marker gene sequencing data and a database of reference genomes. The analysis showed that hydromorphone induces functional phenotypic alterations in gut microbiota in DSS-treated mice, which results in loss of protective and rise of harmful bacterial species. There was decrease in anaerobic bacterial population [Figure 6A], and significant decrease in Gram-positive bacterial population [Figure 6B] was observed in hydromorphone plus DSS-treated mice compared with control mice. Furthermore, there was a significant increase in facultative anaerobic [Figure 6C], Gram-negative [Figure 6D], pathogenic [Figure 6E], mobile genetic elements [MGEs]-containing [Figure 6F], biofilm-forming [Figure 6G], and stress tolerant bacteria [Figure 6H] in hydromorphone plus DSS-treated group compared with control and other treatment groups.

3.9. Hydromorphone in combination with DSS upregulates mu opioid receptor and toll-like receptor expression

Recent studies show increased expression of mu opioid receptor [MOR] and its implications in DSS-induced colitis[38] and IBD.[39] Hydromorphone is a derivative of morphine, which mediate its effects via MOR. Therefore, we determined whether hydromorphone and DSS treatment increase expression of MOR in colonic tissues of mice. Total RNA was isolated from these cells and processed for qPCR. Our results showed that combination of hydromorphone plus DSS treatment significantly increased mRNA levels of MOR [Figure 7A] compared with control. Previous studies from our laboratory have shown that morphine-induced gut microbial dysbiosis and bacterial translocation are mediated by TLR signalling.[3] To determine whether TLR expression on colonic cells is a potential mechanism by which hydromorphone and DSS modulate barrier function, we measured TLR2 and TLR4 expression on colonic cells by qPCR. Results showed that combination of hydromorphone plus DSS treatment significantly upregulated mRNA levels of TLR2 [Figure 7B] and TLR4 [Figure 7C] compared with control, which was consistent with observed human studies.[40,41]

3.10. Hydromorphone modulates intestinal tight junction proteins organisation in an MLCK-dependent manner

Previous studies have demonstrated an association between TLR activation and disruption of tight junction protein organisation in

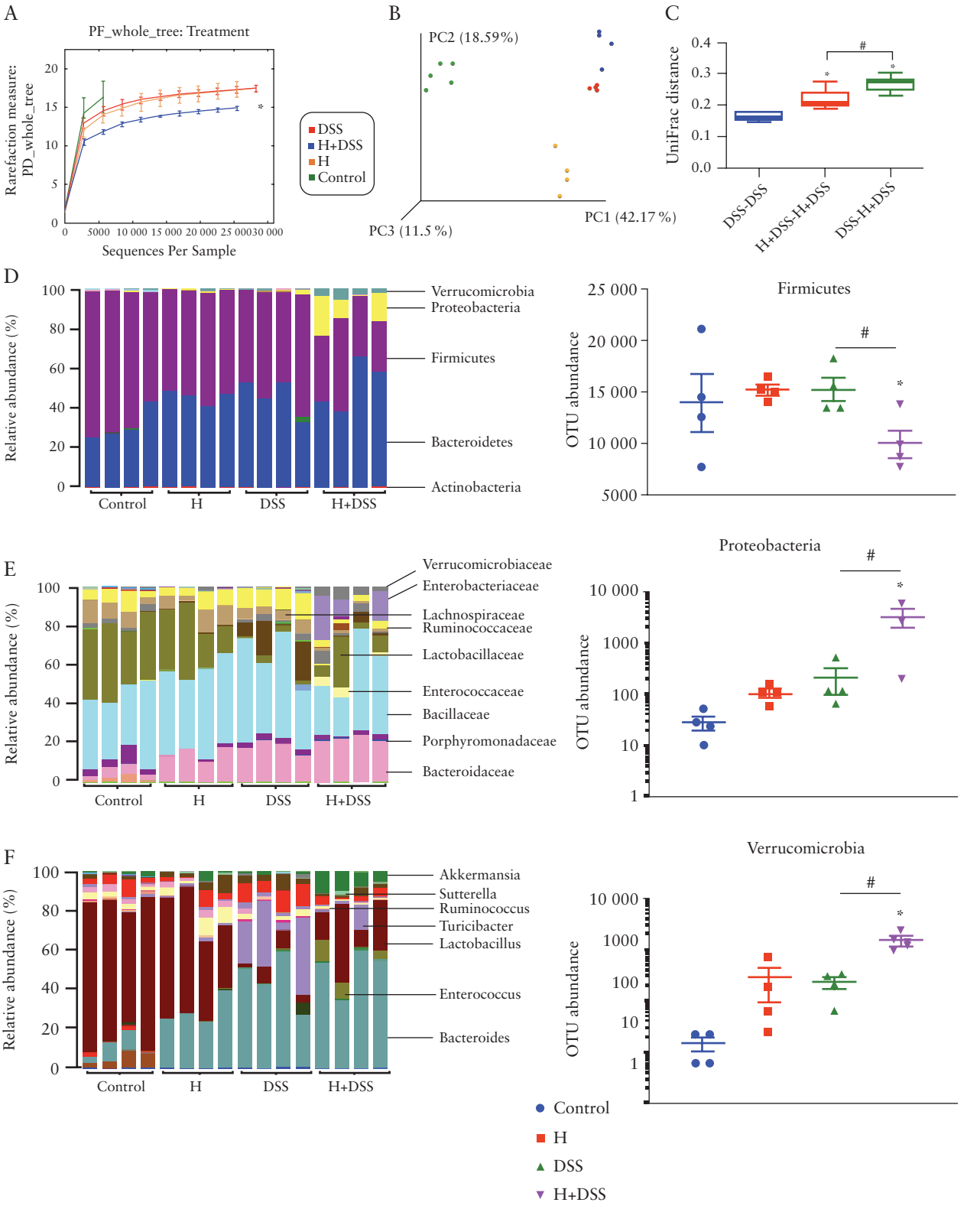

Figure 5. Hydromorphone induces microbial dysbiosis in DSS-treated mice. Sample DNA was extracted from intestinal content of treated and untreated mice. [A] Alpha-diversity analysis shows significant reduction in bacterial speciesrichness or diversity in H + DSS-treated mice [n = 4 per group]. [B] Beta-diversity analysis shows distinct bacterial species distribution between treatment groups [n = 4 per group]. [C] UniFrac distance analysis shows significant distance between treatment groups; 16S rRNA gene sequencing analysis of faecal microbial taxa at the [D] phylum level and OTU abundance of phyla shows the number of OTUs corresponding to the three more abundant and altered phyla [n = 4 per group]. Microbial composition at the [E] family and [F] genus levels [n = 4 per group]. Data show the total identified sequences obtained from each mouse. Mean ± SEM, 95% CI. Asterisk [*] indicates statistical significance [p <0.05] vs control group and hash sign [#] indicates statistical significance [p <0.05] between treatment groups by ANOVA followed by Tukey's multiple comparisons test. DSS, dextran sulphate sodium; OUT, operational taxonomic units; SEM, standard error of the mean; CI, confidence interval; ANOVA, analysis of variance.

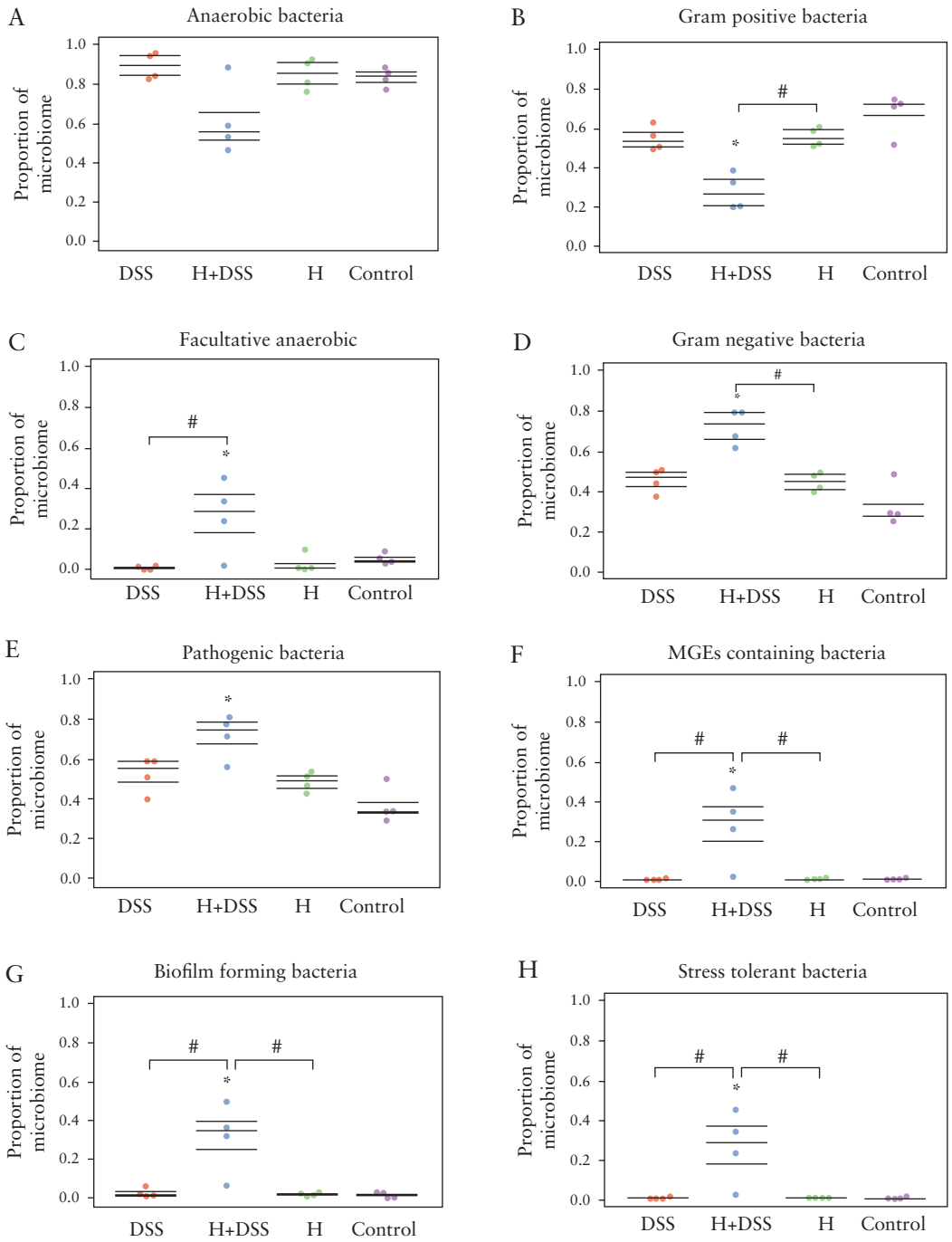

Figure 6. Hydromorphone induces functional phenotypic alterations in gut microbiota in DSS-treated mice. Predicted metagenomic functional analysis was performed by using BugBase software package. Hydromorphone plus DSS treatment results in decrease in [A] anaerobic bacteria, and [B] Gram-positive bacteria, whereas significant increase in [C] facultative anaerobic, [D] Gram-negative, [E] pathogenic, [F] MGEs-containing, [G] biofilm-forming, and [H] stress tolerant bacteria [$n = 4$ per group]. Mean ± SEM, 95% CI. Asterisk [*] indicates statistical significance [$p < 0.05$] vs control group and hash sign [#] indicates statistical significance [$p < 0.05$] between treatment groups by ANOVA followed by Tukey's multiple comparisons test. DSS, dextran sulphate sodium; MGEs, mobile genetic elements; SEM, standard error of the mean; CI, confidence interval; ANOVA, analysis of variance.

the small intestine, which results in gut barrier dysfunction, bacterial translocation, and inflammation.[3,42] Similarly, our findings showing significantly increased expression of TLRs in the large intestine of hydromorphone plus DSS-treated mice prompted us to study the role of tight junction proteins disruption as a potential mechanism. Our results show that in the control group, the paracellular tight junction protein ZO-1 localised on the apical side of the membrane with a continuous and intact organisation. In contrast H- and DSS-treated groups, either alone or in combination, showed disturbed and disorganised localisation of ZO-1 with loss of bright green spots. The smooth arc-like ZO-1 changed into a complex series of rough undulations with thinner and more serpentine morphology, suggesting impaired recruitment of the protein to the membrane [Figure 8A]. The trans-membrane protein claudin-1 also

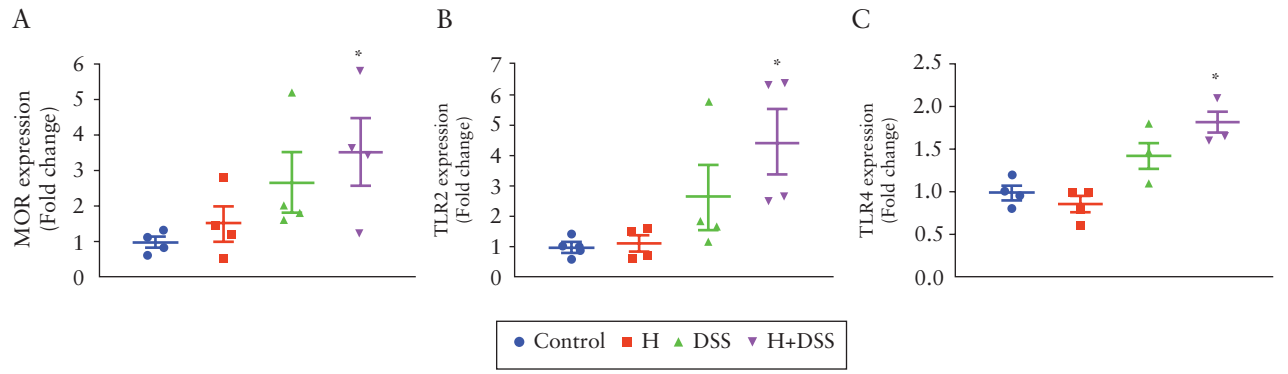

Figure 7. Hydromorphone in combination with DSS upregulates MOR and TLRs expression and determine mRNA levels of [A] MOR expression [$n = 4$ per group], [B] TLR2 expression [$n = 4$ per group], and [C] TLR4 expression using qPCR [$n = 4$ per group]. Analysis was done as described in materials and methods. Mean ± SEM, 95% CI. Asterisk [*] indicates statistical significance [$p < 0.05$] vs control group and hash sign [#] indicates statistical significance [$p < 0.05$] between treatment groups by ANOVA followed by Tukey's multiple comparisons test. DSS, dextran sulphate sodium; MOR, mu opioid receptor; TLR, Toll-like receptor; qPCR, quantitative polymerase chain reaction; SEM, standard error of the mean; CI, confidence interval; ANOVA, analysis of variance.

localised on the apical side of the epithelium in control mice; however, its organisation was seen to be disrupted in mice treated with H and DSS either alone or in combination [Figure 8B]. Our results indicate that hydromorphone treatment affects the distribution and organisation of tight junction proteins, resulting in increased intestinal permeability. Quantification of green fluorescence also showed significant reduction of ZO-1 [Figure 8A] and claudin-1 [Figure 8B] in groups treated with hydromorphone and DSS either alone or in combination.

We next determined the mechanism of how modulation of TLR expression by hydromorphone disrupts tight junction proteins organisation. Recent studies have shown that activation of MLCK induces phosphorylation of MLC, resulting in the internalisation of tight junction proteins such as ZO-1 and claudin-1.[30,43] To validate the role of MLCK in tight junction modulation, animals were injected with ML-7 [2 mg/kg bid], a selective MLCK inhibitor, before hydromorphone and DSS treatment. Disruptions of ZO-1 and claudin-1 were significantly decreased in the groups treated withhydromorphone and DSS, either alone or in combination,and pre-treated with ML-7; and organisation of tight junction proteins was similar to that in the control group [Figure 8A, B].

3.11. MLCK inhibition with ML-7 attenuates hydromorphone-induced severity of colitis in DSS-treated mice

We next asked whether inhibition of MLCK activity by ML-7 attenuates the detrimental effects of hydromorphone on clinical symptoms of colitis and severity of the disease in a mouse model of IBD. The effect of ML-7 on symptoms of colitis was evaluated in an independent experiment in which the effect of hydromorphone on DSS-induced colitis was reproduced, with similar results as described previously [Figures 2 and 3]. We demonstrated that inhibition of MLCK activity by ML-7 resulted in attenuated severity of colitis in the H plus DSS-treated group [Figure 9].

First, we measured the body weight loss and found that hydromorphone and DSS in combination showed significant weight loss scored at 4.90 ± 0.10 [95% CI 4.62–5.18, $p < 0.0001$] compared with DSS alone, which was significantly reversed by ML-7 treatment in the hydromorphone plus DSS group at 7.12 ± 0.21 [95% CI 6.59–7.71, $p < 0.0001$] [Figure 9A]. The colon length of all mice in each group was measured in centimetres and the representative images of colon length are shown in Figure 9B. All DSS-treated animals showed significant colon length shortening. A significant decrease in colon length was observed in the DSS alone and the hydromorphone plus DSS-treated groups at 4.90 ± 0.10 [95% CI 4.62–5.18, $p < 0.0001$] compared with control and individual treatment groups, which was significantly reversed by ML-7 treatment in the hydromorphone plus DSS group at 7.12 ± 0.21 [95% CI 6.53–7.71, $p < 0.0001$] [Figure 9B].

Next, we evaluated bacterial translocation in the liver. The DSS and the hydromorphone plus DSS groups showed significant bacterial translocation compared with control, which was also reduced significantly by ML-7 treatment. The number of CFU was markedly higher in the H plus DSS-treated group at 743 ± 50.69 [95% CI 602.3–883.7, $p < 0.0001$] than that in the control and separately treated groups, which was significantly reduced by ML-7 treatment at 86 ± 33.26 [$p < 0.0001$] [Figure 9C]. The results indicated that ML-7 treatment protects the intestinal mucosal barrier in the murine IBD model, particularly in the context of opioid treatment. In histological evaluation, histological score was significantly higher in groups treated with H and DSS either alone or in combination at 5.52 ± 0.30 [95% CI 4.69–6.36, $p < 0.0001$] compared with control and separately treated groups. Moreover, the protective effects of MLCK inhibitor ML-7 were significantly marked in ML-7 treated groups at 1.56 ± 0.20 [95% CI 1.02–2.12, $p < 0.0001$], which showed normal appearance with little damage or inflammation compared with the control group [Figure 9D].

We next asked whether ML-7 treatment attenuates hydromorphone-induced cytokines production in DSS-treated mice. The hydromorphone plus DSS-treated group displayed significantly elevated levels of IL-6 at 72.57 ± 4.02 [95% CI 61.40–83.73, $p < 0.0001$] [Figure 9E] and IL-17A at 144.9 ± 6.35 [95% CI 127.3–162.6, $p < 0.0006$] [Figure 9F] compared with DSS alone. The level of cytokines was significantly lower in ML-7 treated groups.

4. Discussion

The aim of this study was to evaluate the consequences of opioid exposure on severity of IBD. Several clinical reports indicate increased morbidity and mortality in IBD patients who are on opioids.[22,23] However, it is not clear if these patients require opioids because of greater underlying inflammation, or opioid use drives inflammation leading to greater complications. To determine if opioid use is driving the increased severity of IBD, we investigated

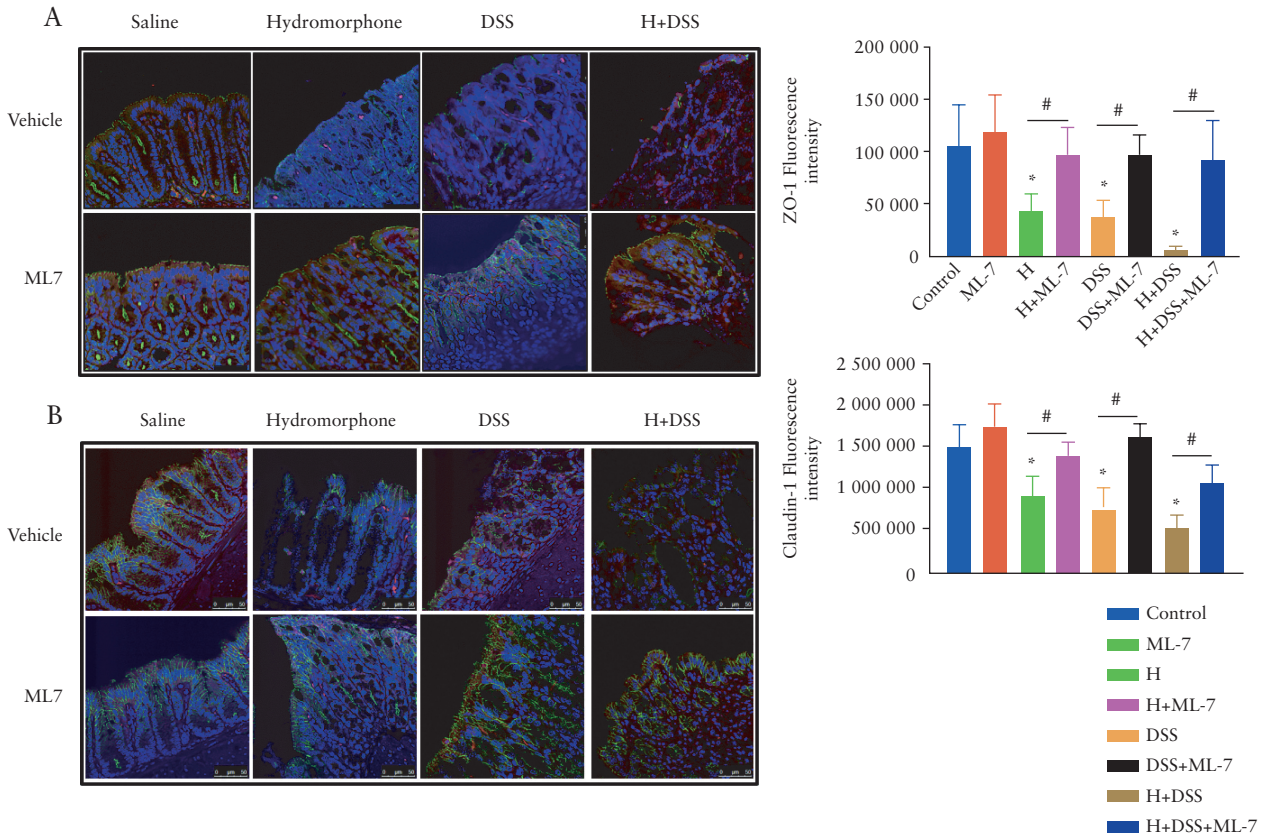

Figure 8. Hydromorphone modulates intestinal tight junction proteins organisation in an MLCK-dependent manner. [A] Representative images of ZO-1 and [B] Claudin-1 organisation in colon sections and quantitative measurement of green fluorescence intensity [$n = 5$ per group] using ImageJ software. Images were analysed by confocal scanning microscope. Scale bar: 50 μm [original magnification: x 40]. Analysis was done as described in materials and methods. Mean ± SEM, 95% CI. Asterisk [*] indicates statistical significance [$p < 0.05$] vs control group and hash sign [#] indicates statistical significance [$p < 0.05$] between treatment groups by ANOVA followed by Tukey's multiple comparisons test. MLCK, myosin light chain kinase; SEM, standard error of the mean; CI, confidence interval; ANOVA, analysis of variance.

the effects of hydromorphone on the severity of the disease in both a DSS colitis and a spontaneous colitis murine model of IBD, by evaluating clinical symptoms of colitis. Our results show that the use of hydromorphone exacerbated colitis in both mouse models of IBD.

In the DSS mouse model, we show that using lower concentration of DSS [3%] for a short duration [5 days] induces milder acute colitis, which is a more relevant model for studying the impact of opioid on the severity of colitis. It is well established that DSS induces inflammation by disrupting the intestinal epithelial barrier and allowing the dissemination of bacteria and their products into the peripheral tissues. The hydromorphone-treated mice showed significant bacterial translocation compared with control mice. The translocation of bacteria was further increased in the animals that were treated with combination of hydromorphone and DSS when compared with control and individually treated groups. We and several other investigators have demonstrated bacterial translocation, septicaemia and gut leakiness in mouse models of opioid treatment.[3,44–46] More recently, several human studies also recapitulate these early studies in rodent models.[47,48] Here we show that hydromorphone treatment further increased DSS-induced damage [Figure 3]. The clinical symptoms were associated with the presence of significant increase in histological damage in hydromorphone plus DSS-treated mice. Our observed clinical symptoms are consistent with previous studies showing shortening of the colon, characteristic intestinal histology, and increase in inflammatory infiltrate of immune cells leading to pro-inflammatory cytokine production.[12,49]

We next validated the consequences of hydromorphone administration in a spontaneous colitis mouse model of IBD. Several studies have shown that the IL-$10^{-/-}$ mouse is a remarkable model because of similarities in various immunological and pathological features to human IBD.[50,51] IL-10 is a regulatory cytokine, and loss of the controlling functions of IL-10 in respect to immune responses against intestinal bacterial antigens leads to the development of spontaneous colitis. IL-$10^{-/-}$ mice raised in conventional facilities develop colitis due to gut barrier dysfunction and abnormal immune response, which initially become evident by weight loss and anaemia.[52]

Our studies with the spontaneous colitis model validated our observations seen with the DSS colitis model. We demonstrated that hydromorphone treatment induced significant body weight loss, bacterial translocation, and intestinal and systemic inflammation in IL-$10^{-/-}$ mice compared with control mice [Figure 4]. Treatment of IL-$10^{-/-}$ mice with hydromorphone induced increased gut permeability, which resulted in dysregulated immune response against gut bacterial antigens which further led to accelerated colitis. Our findings are consistent with previous studies showing that increased gut barrier dysfunction facilitates enteric antigen-induced immune cells activation, leading to uncontrolled pro-inflammatory response which contributes to the development of colitis in IL$10^{-/-}$ mice.[53–55]

We and others have shown that both DSS-induced colitis and spontaneous colitis mouse models resemble IBD in humans because

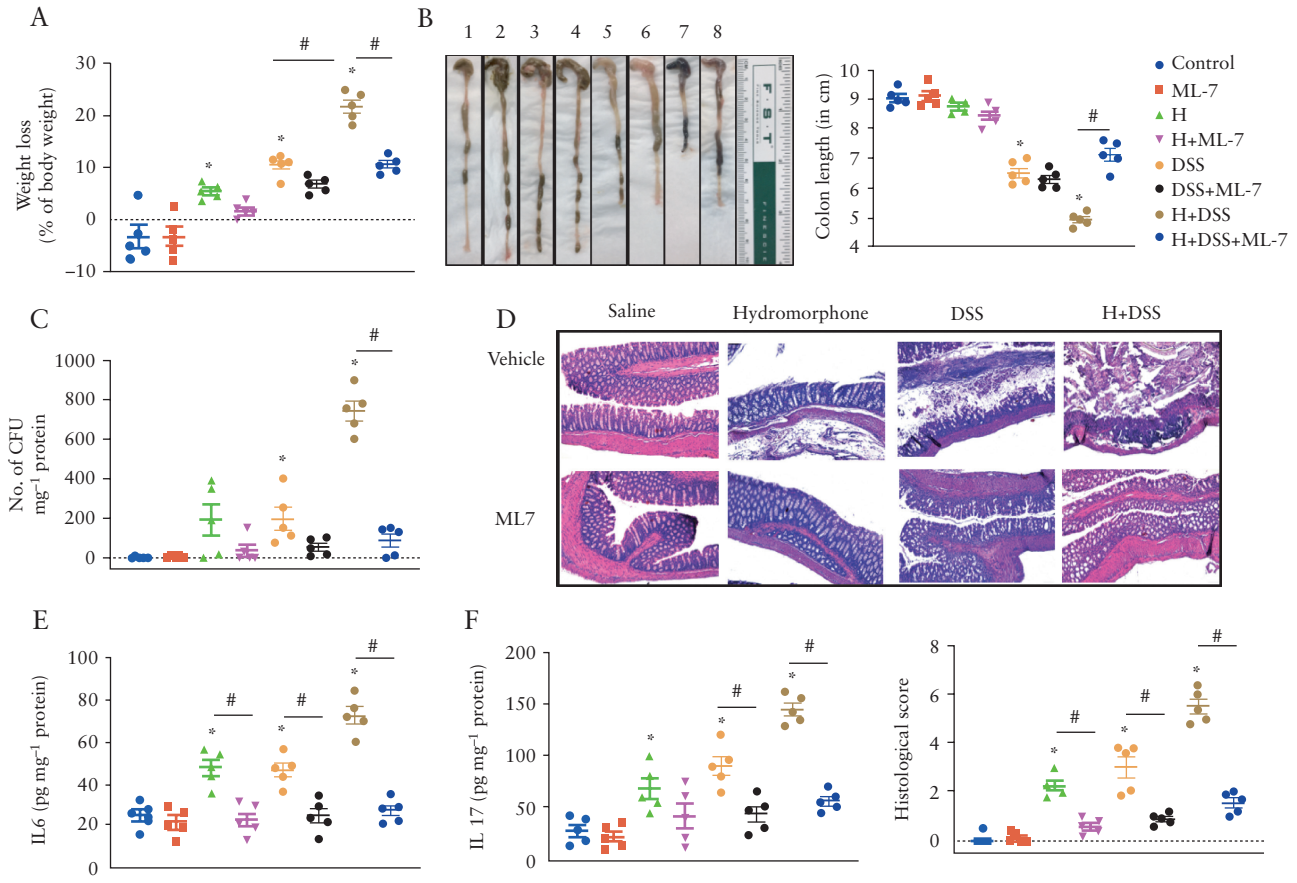

Figure 9. MLCK inhibition with ML-7 attenuates hydromorphone [H]-induced severity of colitis in DSS-treated mice. [A] Changes in body weight [*n* = 5 per group]. [B] Colon length shortening. Representative images of the colon from each group [1]. Control, [2]. ML-7, [3]. Hydromorphone, [4]. H + ML-7, [5]. DSS, [6]. DSS + ML-7, [7]. H + DSS, [8]. H + DSS + ML-7, and colon length was measured [*n* = 5 per group]. [C] Bacterial translocation [*n* = 5 per group]. [D] Representative images of H&E-stained sections of the colon from control and treated mice. Scale bar: 50 μm [original magnification: x 20] [*n* = 5 per group]. Histological scoring was done based on different histopathological features and histopathological changes were scored in a blinded fashion by a pathologist. [E]The concentrations of IL-6 [*n* = 5 per group] and [F] IL-17 in the liver homogenate were measured using ELISA [*n* = 5 per group]. Mean ± SEM, 95% CI. Asterisk [*] indicates statistical significance [$p < 0.05$] vs control group and hash sign [#] indicates statistical significance [$p < 0.05$] between treatment groups by ANOVA followed by Tukey's multiple comparisons test. MLCK, myosin light chain kinase; DSS, dextran sulphate sodium; H&E, haematoxylin and eosin; ELISA, enzyme-linked immunosorbent assay; SEM, standard error of the mean; CI, confidence interval; ANOVA, analysis of variance.

of several similar features, such as clinical symptoms, gut barrier dysfunction, altered gut microbiota, inflammatory markers, and histopathological changes.[11] Our findings of opioid use as an indicator of more severe disease are in agreement with previous reports showing that narcotic use is associated with worse disease activity and diminished quality of life in IBD patients.[22] Therefore, based on our results, we conclude that hydromorphone use for pain management increases the severity of IBD.

Next, we show that hydromorphone and DSS treatment independently altered gut microbiota but, in combination, a significantly greater microbial dysbiosis was observed with exacerbation in the severity of colitis. Our analysis shows that microbial dysbiosis resulted mainly in dysfunction of commensal microbiota and increase in pathogenic bacteria [Figure 6]. The healthy gut microbiota is known to be stable over time. However, diseases associated with immune responses drive the microbial community to an unbalanced and unstable state.[56] Our findings of alpha and beta diversity are in agreement with previous reports showing decreased bacterial species richness and distinct microbial communities after induction of colitis.[57,58] Normally in a healthy gut, the most abundant phyla Firmicutes and Bacteroidetes dominate the microbial community, and Proteobacteria, Verrucomicrobia, Actinobacteria, and TM7 are less abundant. Our taxonomic analysis shows that the dominant bacterial species were drastically altered, which was characterised by a significant decrease in Firmicutes and an increase in the relative abundance of Proteobacteria and Verrucomicrobia in hydromorphone plus DSS-treated animals, which is consistent with other reports in IBD patients.[58,59] We observed significant differences between hydromorphone and non-hydromorphone groups at the taxonomic level after induction of colitis, and found that specific taxa were associated with these groups. Of interest, Bacteroides, Enterococcus, Sutterella, and Akkermansia were enriched, whereas Lactobacillus and Lachnospiraceae were decreased in the hydromorphone group before induction of colitis, indicating their strong association with hydromorphone exposure. The changes in abundance of these bacteria at phylum and genus levels were markedly increased in the hydromorphone plus DSS treatment group. Therefore, we speculate that hydromorphone-induced changes in these taxa may have specific roles in the susceptibility and severity of DSS-induced colitis. The expansion of Sutterella is associated with the degradation of secretory IgA and mucosal damage.[58] The enriched level of *Akkermansia muciniphila*, a putative host-derived mucin degrader, has been linked with inflammation and contribution

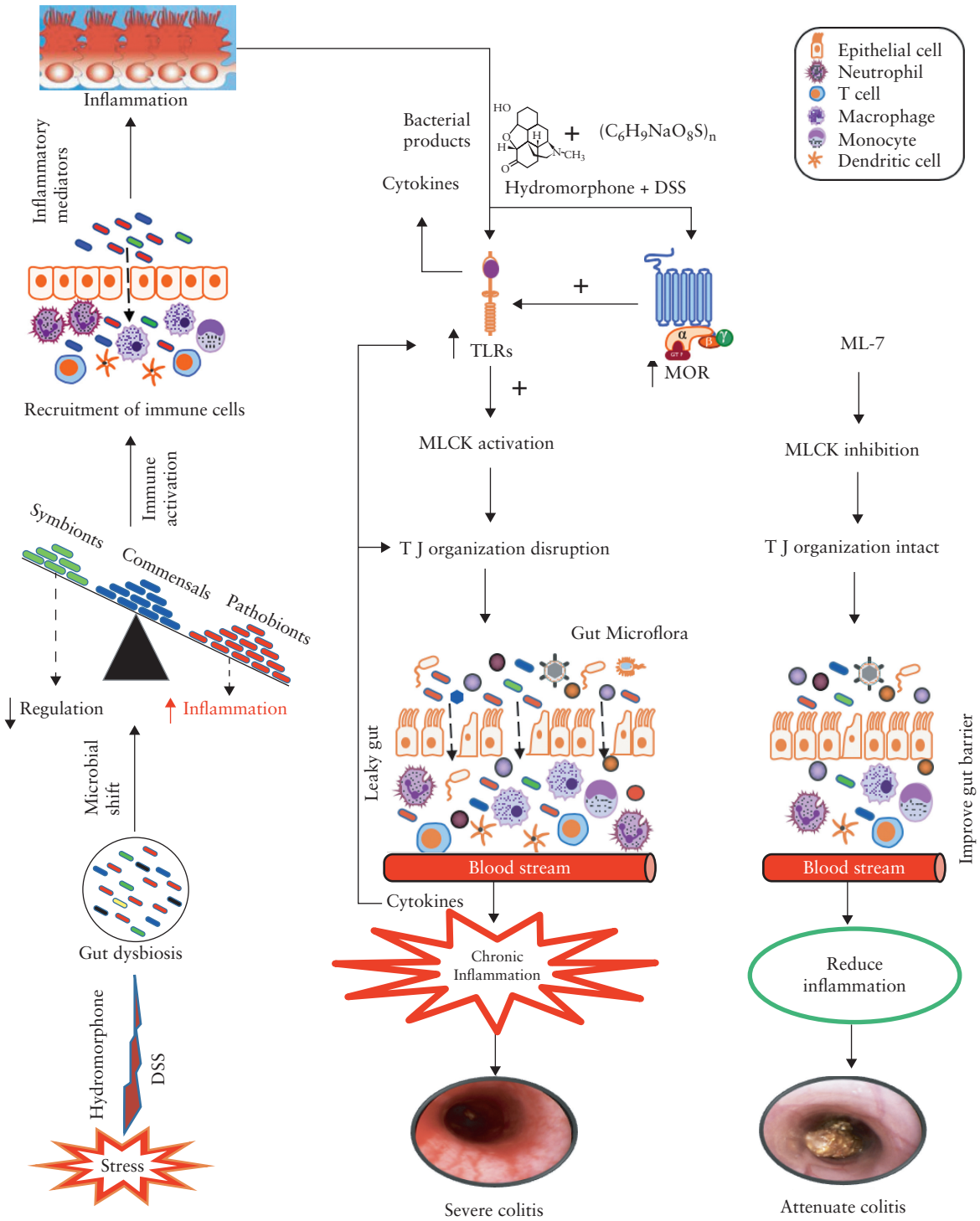

Figure 10. ML-7 treatment attenuates hydromorphone-induced severity of colitis in mice. Schematic illustration of prescription opioid, hydromorphone,-induced gut microbial dysbiosis and immune dysfunction, and thus enhanced disease severity, which is attenuated in ML-7 treated group in a murine model of inflammatory bowel disease [IBD].

to exacerbation of colitis.[24] The expansion of Proteobacteria is associated with intestinal inflammation.

Our predicted metagenomic functional analysis showed significant increase in pathogenic, MGEs-containing, biofilm-forming, facultative anaerobic and Gram-negative bacteria, while showing a decrease in anaerobic and Gram-positive bacteria in hydromorphone plus DSS-treated mice compared with all other groups. Studies have shown that pathogenic bacteria promote their development and virulence by using nutrients and regulatory signals produced by commensal microbiota, thereby promoting infection.[60] Biofilm-forming bacteria adhere to the surface and increase their metabolic efficiency. Expansion in biofilm-forming and MGEs-containing bacteria offer horizontal gene transfer, produce toxins, and show enhanced resistance to phagocytosis and antimicrobial agents.[61–63]

Proteobacteria, especially Enterobacteriaceae, can cause metabolic dysfunctions of the microbiota and affect the production of bacterial by-products such as short-chain fatty acids [SCFAs], thus affecting mucosal immune response.[56] The mucosal inflammatory environment favours the growth of Gram-negative facultative anaerobes Proteobacteria at the cost of obligate anaerobes Firmicutes. Enterobacteriaceae can use oxygen or nitrate for their aerobic and anaerobic respiration, respectively. Thus, expansion of these communities outcompetes commensal bacteria by reducing the availability of oxygen[64] and depletes Firmicutes that depend on fermentation for their development.[56] Enterobacteriaceae are also known to possess MGEs, which are responsible for genetic variability and gene transfer in bacterial strains and might contribute to their strength to outcompete other commensal gut microbiota.[56] The above findings indicate that hydromorphone-treated commensal gut microbiota might be less likely to outcompete pathogenic bacteria and prevent their colonisation in the gut of DSS-treated mice. Based on the above findings, we propose that an increased prevalence of Proteobacteria and Verrucomicrobia may be a useful diagnostic signature marker of dysbiosis and severity of IBD.

It is still unclear whether alterations in the gut microbial composition represent the cause or consequence of host inflammation and state of the disease. Hydromorphone-induced changes in gut microbiota are crucial determinants in the susceptibility to experimental colitis in a murine model of IBD. The mechanism by which hydromorphone induces microbial dysbiosis and exacerbates severity of colitis is not fully clear. Here we show that microbial dysbiosis is also associated with mobilisation of inflammatory immune cells into the colon [Figure 3D], which play an important role in production of cytokines and thus in inflammation. Recent studies have also shown the association of increased MOR expression with IBD, through increased migration of circulatory immune cells to the site of inflammation,[2,39] which is consistent with our findings. Based on these results, we speculate that hydromorphone plus DSS treatment may exert its immune-modulatory effects via MOR signalling. The role of TLRs is well established in mucosal pathogenic complications. Our laboratory and others have shown that opioid[3,34] and DSS can stimulate TLRs and modulate tight junction proteins, leading to a disrupted epithelial barrier which results in gut permeability and subsequent inflammation.[65] In the present study we found higher levels of TLR2 and TLR4 expression consistent with previous studies showing high levels of TLR expression in colon biopsy of IBD patients[40,41] and in DSS-treated mice.[66,67] In our study, TLR2 expression level was higher compared with TLR4 expression. The possible reason could be that TLR2 interacts with peptidoglycan, a component of all bacterial cell walls, as well as additional constituents of Gram-positive bacteria and fungi. A recent study also demonstrated that Gram-positive bacteria trigger colitis by inducing monocyte/macrophage recruitment into the colon,[19] which is similar to our findings. Our results indicate that hydromorphone, a MOR selective ligand, plays a role in the progression of DSS-induced colitis through activation of MOR and TLRs signalling pathways. We can hypothesise that both hydromorphone and DSS alter gut microbial composition, which initiates recruitment and local proliferation of immune cells into the colon to create an inflammatory environment, which results in increased gut permeability and bacterial translocation.

We show strong relationship between increase in TLR expression and disruption of tight-junction proteins organisation in the intestine, which is consistent with previous observations.[3,42] Tight junction proteins have been shown to seal the space between gut epithelial cells and play a key role in blocking potential pathogen invasion. Distribution of tight junction proteins is involved in modulating intestinal permeability. Therefore, we determine intestinal epithelial tight junction protein expression in this study. We show that hydromorphone treatment significantly disrupted tight junction proteins organisation in gut epithelial cells, which resulted in compromised intestinal barrier function, bacterial translocation, and inflammation. We speculate that increased intestinal inflammation and pro-inflammatory cytokines play a feedback role in the intestinal epithelium, activating the MLCK signalling pathway to cause further barrier dysfunction and thus increasing the severity of colitis. Some of the reports have shown that an increased intestinal permeability was partly regulated by MLCK upregulation and increasing phosphorylation of MLC.[42,43] Therefore, we evaluated the effect of MLCK inhibitor ML-7 on the detrimental effect of hydromorphone on severity of DSS-induced colitis. The administration of ML-7 prevented intestinal barrier dysfunction by inhibiting MLCK protein expression and increasing intestinal epithelial tight junction expression. We also show that ML-7 treatment ameliorated the clinical symptoms of colitis including weight loss, colon length shortening, histological intestinal damage, and inflammation in groups treated with H and DSS either alone or in combination. These results indicate that the beneficial effects of ML-7 on the intestinal mucosal barrier may suppress the intestinal inflammatory pathology and consequently attenuate colonic inflammation.

The impaired intestinal barrier function and inflow of commensal bacteria are prerequisites for chronic inflammation, which results in increased severity of DSS-induced colitis. We show that the severity of colitis was significantly attenuated by selective inhibition of MLCK activation using ML-7 treatment [Figure 10]. The results of this study suggest that use of opioids for pain management is a risk factor in the comorbidities associated with IBD, as opioid potentially alters the gut microbiome. The restoration of gut homeostasis by modulating the gut microbiota could be a relevant therapeutic strategy. These findings warrant a careful evaluation of the potential detrimental effects of prescription opioids on IBD severity, and suggest that opioids should be prescribed cautiously.

Funding

This work was supported in part by the National Institute for Drug Abuse [NIDA] and National Institutes of Health [NIH] grants [grant numbers R01 DA043252, R01 DA037843, K05 DA033881, R01 DA044582, R01 DA034582] to SR; the American Society of Colon and Rectal Surgeons [ASCRS] for General Surgery Resident Research award [GSRRIG-026] to RO; and a Miami-Center for AIDS Research [CFAR] for pilot research grant award [GR010993] to US.

Conflict of Interest

The authors have declared that no conflict of interest exists.

Acknowledgments

We thank Dr Feng Bai, pathologist, for helping in histological and colonoscopic evaluation.

Author Contributions

US designed and performed the experiments, acquisition of data, analysis and interpretation of data, andstatistical analysis, and wrote the manuscript with final approval of the version to be published. RO contributed to acquisition of dataand analysis, and obtained funding and final approval of the version

to be published. FE, LZ, JM, and MS helped in experiments, ordering all the required chemicals, reagents, and animals, and in final approval of the version to be published. SB helped in microbiome data analysis and in final approval of the version to be published. BS and SR supervised development of the work and provided guidance and final approval of the version to be published. AS contributed general, material, administrative support, manuscript evaluation, and final approval of the version to be published. MA helped in data interpretation, critical revision of the manuscript for important intellectual content, and final approval of the version to be published. SR contttributed to the study concept, designed experiments, obtained funding, and helped in data interpretation, study supervision, critical revision of the manuscript for important intellectual content, and final approval of the version to be published.

References

1. Manchikanti L, Fellows B, Ailinani H, Pampati V. Therapeutic use, abuse, and nonmedical use of opioids: a ten-year perspective. *Pain Physician* 2010;**2000**:401–35.
2. Roy S, Ninkovic J, Banerjee S, *et al*. Opioid drug abuse and modulation of immune function: Consequences in the susceptibility to opportunistic infections. *J Neuroimmune Pharmacol* 2011;**6**:442–65. Doi
3. Meng J, Yu H, Ma J, Wang J, *et al*. Morphine induces bacterial translocation in mice by compromising intestinal barrier function in a TLR-dependent manner. *PLoS One* 2013;**8**:54040.
4. Crohn's & Colitis Foundation of America. The facts about inflammatory bowel diseases. *Inflamm Bowel Dis* 2014;**2**:1.
5. Xavier RJ, Podolsky DK. Unravelling the pathogenesis of inflammatory bowel disease. *Nature* 2007;**448**:427–34.
6. Kaser A, Zeissig S, Blumberg RS. Genes and environment: how will our concepts on the pathophysiology of IBD develop in the future? *Dig Dis* 2010;**28**:395–405.
7. Prideaux L, Kamm MA, De Cruz PP, Chan FK, Ng SC. Inflammatory bowel disease in Asia: a systematic review. *J Gastroenterol Hepatol* 2012;**27**:1266–80.
8. M'Koma AE. Inflammatory bowel disease: An expanding global health problem. *Clin Med Insights Gastroenterol* 2013;**6**:33–47.
9. Høivik ML, Moum B, Solberg IC, Henriksen M, Cvancarova M, Bernklev T; IBSEN Group. Work disability in inflammatory bowel disease patients 10 years after disease onset: results from the IBSEN Study. *Gut* 2013;**62**:368–75.
10. Netjes JE, Rijken M. Labor participation among patients with inflammatory bowel disease. *Inflamm Bowel Dis* 2013;**19**:81–91.
11. Chassaing B, Aitken JD, Malleshappa M, Vijay-Kumar M. Dextran sulfate sodium [DSS]-induced colitis in mice. *Curr Protoc Immunol* 2014;**104**:1–14.
12. Yan Y, Kolachala V, Dalmasso G, *et al*. Temporal and spatial analysis of clinical and molecular parameters in dextran sodium sulfate induced colitis. *PLoS One* 2009;**4**:e6073.
13. Kozlowski C, Jeet S, Beyer J, *et al*. An entirely automated method to score DSS-induced colitis in mice by digital image analysis of pathology slides. *Dis Model Mech* 2013;**6**:855–65.
14. Perše M, Cerar A. Dextran sodium sulphate colitis mouse model: traps and tricks. *J Biomed Biotechnol* 2012;**2012**:718617.
15. He X, Wei Z, Wang J, *et al*. Alpinetin attenuates inflammatory responses by suppressing TLR4 and NLRP3 signaling pathways in DSS-induced acute colitis. *Sci Rep* 2016;**6**:28370.
16. Axelsson LG, Landström E, Bylund-Fellenius AC. Experimental colitis induced by dextran sulphate sodium in mice: beneficial effects of sulphasalazine and olsalazine. *Aliment Pharmacol Ther* 1998;**12**:925–34.
17. De Fazio L, Cavazza E, Spisni E, *et al*. Longitudinal analysis of inflammation and microbiota dynamics in a model of mild chronic dextran sulfate sodium-induced colitis in mice. *World J Gastroenterol* 2014;**20**:2051–61.
18. Clemente JC, Ursell LK, Parfrey LW, Knight R. The impact of the gut microbiota on human health: an integrative view. *Cell* 2012;**148**:1258–70.
19. Nakanishi Y, Sato T, Ohteki T. Commensal Gram-positive bacteria initiates colitis by inducing monocyte/macrophage mobilization. *Mucosal Immunol* 2015;**8**:152–60.
20. Frank DN, St Amand AL, Feldman RA, Boedeker EC, Harpaz N, Pace NR. Molecular-phylogenetic characterization of microbial community imbalances in human inflammatory bowel diseases. *Proc Natl Acad Sci U S A* 2007;**104**:13780–5.
21. Targownik LE, Nugent Z, Singh H, Bugden S, Bernstein CN. The prevalence and predictors of opioid use in inflammatory bowel disease: a population-based analysis. *Am J Gastroenterol* 2014;**109**:1613–20.
22. Cross RK, Wilson KT, Binion DG. Narcotic use in patients with Crohn's disease. *Am J Gastroenterol* 2005;**100**:2225–9.
23. Burr NE, Smith C, West R, Hull MA, Subramanian V. Increasing prescription of opiates and mortality in patients with inflammatory bowel diseases in England. *Clin Gastroenterol Hepatol* 2018;**16**:534–41.e6.
24. Håkansson Å, Tormo-Badia N, Baridi A, *et al*. Immunological alteration and changes of gut microbiota after dextran sulfate sodium [DSS] administration in mice. *Clin Exp Med* 2015;**15**:107–20.
25. Shin J, Seol I, Son C. Interpretation of animal dose and human equivalent dose for drug development. *J Korean Orient Med* 2010;**31**:1–7.
26. Kumar MG, Lin S. Hydromorphone in the management of cancer-related pain: an update on routes of administration and dosage forms. *J Pharm Pharm Sci* 2007;**10**:504–18.
27. Food and Drug Adminstration. *HIGHLIGHTS OF PRESCRIBING INFORMATION. These highlights do not include all the information needed to use DILAUDID ® ORAL SOLUTION and DILAUDID ® TABLETS safely and effectively*. White Oak, MD: FDA; 2016; 1–31.
28. Sharma V, McNeill JH. To scale or not to scale: the principles of dose extrapolation. *Br J Pharmacol* 2009;**157**:907–21.
29. Keilholz U, Rohde L, Mehlitz P, *et al*. First-in-man dose escalation and pharmacokinetic study of CAP7.1, a novel prodrug of etoposide, in adults with refractory solid tumours. *Eur J Cancer* 2017;**80**:14–25.
30. Liu X, Xu J, Mei Q, Han L, Huang J. Myosin light chain kinase inhibitor inhibits dextran sulfate sodium-induced colitis in mice. *Dig Dis Sci* 2013;**58**:107–14. Doi: 10.1007/s10620-012-2304-3.
31. Márquez L, Pérez-Nievas BG, Gárate I, *et al*. Anti-inflammatory effects of Mangifera indica L. extract in a model of colitis. *World J Gastroenterol* 2010;**16**:4922–31.
32. Hirao LA, Grishina I, Bourry O, *et al*. Early mucosal sensing of SIV infection by paneth cells induces IL-1β production and initiates gut epithelial disruption. *PLoS Pathog* 2014;**10**:e1004311.
33. Gohl DM, Vangay P, Garbe J, *et al*. Systematic improvement of amplicon marker gene methods for increased accuracy in microbiome studies. *Nat Biotechnol* 2016;**34**:942–9.
34. Banerjee S, Sindberg G, Wang F, *et al*. Opioid-induced gut microbial disruption and bile dysregulation leads to gut barrier compromise and sustained systemic inflammation. *Mucosal Immunol* 2016;**9**:1418–28.
35. Langille MG, Zaneveld J, Caporaso JG, *et al*. Predictive functional profiling of microbial communities using 16S rRNA marker gene sequences. *Nat Biotechnol* 2013;**31**:814–21.
36. Caporaso JG, Kuczynski J, Stombaugh J, *et al*. QIIME allows analysis of high-throughput community sequencing data. *Nat Methods* 2010;**7**:335–6.
37. Ward T, Larson JM, Meulemans J, *et al*. BugBase predicts organism-level microbiome phenotypes. *BioRxiv* 2017:1–19. Doi: http://dx.doi.org/10.1101/133462.
38. Anselmi L, Huynh J, Duraffourd C, *et al*. Activation of μ opioid receptors modulates inflammation in acute experimental colitis. *Neurogastroenterol Motil* 2015;**27**:509–23.
39. Philippe D, Chakass D, Thuru X, *et al*. Mu opioid receptor expression is increased in inflammatory bowel diseases: implications for homeostatic intestinal inflammation. *Gut* 2006;**55**:815–23.
40. Szebeni B, Veres G, Dezsõfi A, *et al*. Increased expression of Toll-like receptor [TLR] 2 and TLR4 in the colonic mucosa of children with inflammatory bowel disease. *Clin Exp Immunol* 2008;**151**:34–41.
41. Frolova L, Drastich P, Rossmann P, Klimesova K, Tlaskalova-Hogenova H. Expression of Toll-like receptor 2 [TLR2], TLR4, and CD14 in biopsy samples of patients with inflammatory bowel diseases: upregulated expression of TLR2 in terminal ileum of patients with ulcerative colitis. *J Histochem Cytochem* 2008;**56**:267–74.

42. Guo S, Nighot M, Al-Sadi R, Alhmoud T, Nighot P, Ma TY. Lipopolysaccharide regulation of intestinal tight junction permeability is mediated by TLR4 signal transduction pathway activation of FAK and MyD88. *J Immunol* 2015;**195**:4999–5010.
43. Chen C, Wang P, Su Q, Wang S, Wang F. Myosin light chain kinase mediates intestinal barrier disruption following burn injury. *PLoS One* 2012;**7**:e34946.
44. Hilburger ME, Adler MW, Truant AL, *et al.* Morphine induces sepsis in mice. *J Infect Dis* 1997;**176**:183–8.
45. Meng J, Banerjee S, Li D, *et al.* Opioid exacerbation of gram-positive sepsis, induced by gut microbial modulation, is rescued by IL-17A neutralization. *Sci Rep* 2015;**5**:1–17.
46. Sindberg GM, Sharma U, Banerjee S, *et al.* An infectious murine model for studying the systemic effects of opioids on early HIV pathogenesis in the gut. *J Neuroimmune Pharmacol* 2015;**10**:74–87.
47. Zhang R, Meng J, Lian Q, *et al.* Prescription opioids are associated with higher mortality in patients diagnosed with sepsis: A retrospective cohort study using electronic health records. *PLoS One* 2018;**13**:1–8.
48. Green J. Epidemiology of opioid abuse and addiction. *J Emerg Nurs* 2017;**43**:106–13.
49. Hall LJ, Faivre E, Quinlan A, Shanahan F, Nally K, Melgar S. Induction and activation of adaptive immune populations during acute and chronic phases of a murine model of experimental colitis. *Dig Dis Sci* 2011;**56**:79–89.
50. Strober W, Fuss IJ, Blumberg RS. The immunology of mucosal models of inflammation. *Annu Rev Immunol* 2002;**20**:495–549.
51. Holgersen K, Kvist PH, Markholst H, Hansen AK, Holm TL. Characterisation of enterocolitis in the piroxicam-accelerated interleukin-10 knock out mouse—a model mimicking inflammatory bowel disease. *J Crohns Colitis* 2014;**8**:147–60.
52. Sellon RK, Tonkonogy S, Schultz M, *et al.* Resident enteric bacteria are necessary for development of spontaneous colitis and immune system activation in interleukin-10-deficient mice. *Infect Immun* 1998;**66**:5224–31.
53. Berg DJ, Davidson N, Kühn R, *et al.* Enterocolitis and colon cancer in interleukin-10-deficient mice are associated with aberrant cytokine production and CD4[+] TH1-like responses. *J Clin Invest* 1996;**98**:1010–20.
54. Fiorentino DF, Zlotnik A, Mosmann TR, Howard M, O'Garra A. IL-10 inhibits cytokine production by activated macrophages. *J Immunol* 1991;**147**:3815–22.
55. Kennedy RJ, Hoper M, Deodhar K, Erwin PJ, Kirk SJ, Gardiner KR. Interleukin 10-deficient colitis: new similarities to human inflammatory bowel disease. *Br J Surg* 2000;**87**:1346–51.
56. Shin NR, Whon TW, Bae JW. Proteobacteria: microbial signature of dysbiosis in gut microbiota. *Trends Biotechnol* 2015;**33**:496–503.
57. Munyaka PM, Rabbi MF, Khafipour E, Ghia JE. Acute dextran sulfate sodium [DSS]-induced colitis promotes gut microbial dysbiosis in mice. *J Basic Microbiol* 2016;**56**:986–98.
58. Munyaka PM, Eissa N, Bernstein CN, Khafipour E, Ghia JE. Antepartum antibiotic treatment increases offspring susceptibility to experimental colitis: a role of the gut microbiota. *PLoS One* 2015;**10**:e0142536.
59. He Q, Wang L, Wang F, *et al.* Microbial fingerprinting detects intestinal microbiota dysbiosis in Zebrafish models with chemically-induced enterocolitis. *BMC Microbiol* 2013;**13**:289–304.
60. Bäumler AJ, Sperandio V. Interactions between the microbiota and pathogenic bacteria in the gut. *Nature* 2016;**535**:85–93.
61. Burmølle M, Webb JS, Rao D, Hansen LH, Sørensen SJ, Kjelleberg S. Enhanced biofilm formation and increased resistance to antimicrobial agents and bacterial invasion are caused by synergistic interactions in multispecies biofilms. *Appl Environ Microbiol* 2006;**72**:3916–23.
62. Aparna MS, Yadav S. Biofilms: microbes and disease. *Braz J Infect Dis* 2008;**12**:526–30.
63. Queck SY, Khan BA, Wang R, *et al.* Mobile genetic element-encoded cytolysin connects virulence to methicillin resistance in MRSA. *PLoS Pathog* 2009;**5**:e1000533.
64. Nagao-Kitamoto H, Shreiner AB, Gillilland MG 3rd, *et al.* Functional characterization of inflammatory bowel disease-associated gut dysbiosis in gnotobiotic mice. *Cell Mol Gastroenterol Hepatol* 2016;**2**:468–81.
65. Hernández-Chirlaque C, Aranda CJ, Ocón B, *et al.* Germ-free and antibiotic-treated mice are highly susceptible to epithelial injury in DSS colitis. *J Crohns Colitis* 2016;**10**:1324–35.
66. Heimesaat MM, Fischer A, Siegmund B, *et al.* Shift towards pro-inflammatory intestinal bacteria aggravates acute murine colitis via Toll-like receptors 2 and 4. *PLoS One* 2007;**2**:1–7.
67. Dheer R, Santaolalla R, Davies JM, *et al.* Intestinal epithelial toll-like receptor 4 signaling affects epithelial function and colonic microbiota and promotes a risk for transmissible colitis. *Infect Immun* 2016;**84**:798–810.